RESEARCH ARTICLE

Peptidergic signaling from clock neurons regulates reproductive dormancy in *Drosophila melanogaster*

Dóra Nagy[1], Paola Cusumano[1], Gabriele Andreatta[1], Ane Martin Anduaga[2], Christiane Hermann-Luibl[3], Nils Reinhard[3], João Gesto[2¤], Christian Wegener[3], Gabriella Mazzotta[1], Ezio Rosato[2], Charalambos P. Kyriacou[2]*, Charlotte Helfrich-Förster[3]*, Rodolfo Costa[1]*

1 Department of Biology, University of Padova, Padova, Italy, **2** Department of Genetics and Genome Biology, University of Leicester, Leicester, United Kingdom, **3** Neurobiology and Genetics, Theodor-Boveri-Institute, Biocenter, University of Würzburg, Würzburg, Germany

¤ Current address: Mosquitos Vetores: Endossimbiontes e Interação Patógeno-Vetor, Instituto René Rachou, Fiocruz, Belo Horizonte, MG, Brazil.
* cpk@leicester.ac.uk (CPK); charlotte.foerster@biozentrum.uni-wuerzburg.de (CHF); rodolfo.costa@unipd.it (RC)

Abstract

With the approach of winter, many insects switch to an alternative protective developmental program called diapause. *Drosophila melanogaster* females overwinter as adults by inducing a reproductive arrest that is characterized by inhibition of ovarian development at previtellogenic stages. The insulin producing cells (IPCs) are key regulators of this process, since they produce and release insulin-like peptides that act as diapause-antagonizing hormones. Here we show that in *D. melanogaster* two neuropeptides, Pigment Dispersing Factor (PDF) and short Neuropeptide F (sNPF) inhibit reproductive arrest, likely through modulation of the IPCs. In particular, genetic manipulations of the PDF-expressing neurons, which include the sNPF-producing small ventral Lateral Neurons (s-LN$_v$s), modulated the levels of reproductive dormancy, suggesting the involvement of both neuropeptides. We expressed a genetically encoded cAMP sensor in the IPCs and challenged brain explants with synthetic PDF and sNPF. Bath applications of both neuropeptides increased cAMP levels in the IPCs, even more so when they were applied together, suggesting a synergistic effect. Bath application of sNPF additionally increased Ca^{2+} levels in the IPCs. Our results indicate that PDF and sNPF inhibit reproductive dormancy by maintaining the IPCs in an active state.

Author summary

Diapause is a hormonally mediated process that allows insects to predict and respond to unfavourable conditions by altering their metabolism and behavior to resist the oncoming environmental challenges. In *Drosophila melanogaster* females a protective state of reproductive dormancy is induced by lower temperatures and shorter photoperiods that mimic

the approach of winter. By genetically manipulating the circadian pacemaker s-LN$_v$s cells, which express two neuropeptides, Pigment dispersing factor (PDF) and short Neuropeptide F (sNPF), we were able to modulate levels of gonadal arrest. PDF and sNPF appear to act as antagonists to dormancy, as do the Drosophila insulin-like peptides (dILPs) that are expressed in the insulin producing cells (IPCs). Indeed, we observe that the axonal projections from the s-LNvs appear to overlap with those from the IPCs implying that the clock cells signal to the IPCs. We confirm this possible communication by applying the two synthetic peptides to the IPCs and detecting a response in the IPC signal transduction pathway. We conclude that the clock neurons activate the IPCs via PDF and sNPF, which in turn release the dILPs, antagonise dormancy and lead to reproductive growth, thereby uncovering a neurogenetic circadian-overwintering axis.

Introduction

To synchronize with the Earth's rhythmic environment, most higher organisms have evolved endogenous time-keeping systems [1,2]. While the highly conserved circadian clock is well-characterized [3,4], our knowledge of the seasonal clock that governs the overwintering response (diapause) in insects is still fragmentary [5,6]. Diapause refers to an alternative developmental program, typically induced by the shortening days and falling temperatures of the approaching winter [1,7]. Diapausing animals are characterized by low metabolic rate, drastically decreased food intake, extended lifespan, and increased stress resistance [8–15]. The fruit fly *Drosophila melanogaster* exhibits an adult reproductive 'diapause' manifested by arrested ovarian development which is stimulated by low temperatures and can be enhanced by short photoperiods [15,16]. While the *Drosophila* literature refers to this phenomenon as 'diapause' rather than 'dormancy' or 'overwintering', we recognize that it is not a classic photoperiodically-induced state because it requires cold-temperature to induce the reproductive quiescence. Nevertheless, it shows features that are commonly associated with responses that are resistant to environmental stresses [7,15,16].

An increasing body of evidence suggests that insulin-like signaling is a key regulator of diapause in numerous species [13,17–20]. In *Drosophila*, 4 of the 8 identified insulin-like proteins (DILP1, -2, -3, -5) are produced in 14 median neurosecretory cells (designated as Insulin Producing Cells, IPCs) of the *Pars intercerebralis* (PI), which are anatomically connected to the key neuroendocrine system that governs hormonal regulation of gonadal arrest [21–25]. Even though the center for dormancy control is believed to be in the PI [26–28], the neurosecretory cells in this brain area, including the IPCs, do not have a circadian clock, and would therefore have to receive any timing information (if any) from other cells [29–33]. A challenging question is how the environmental signals that trigger dormancy (i.e. decreasing photoperiod and temperature) including putative timing information, are perceived, interpreted, and converted into hormonal signals in the brain, leading to the overwintering phenotype [34].

Even though several neuropeptides, neurotransmitters, and peptide hormones have already been identified as modulators of function of the IPCs (reviewed in [35,36]), there are still gaps in our understanding of how the activity of these cells is controlled. Recent research revealed a synaptic connection between the IPCs and one group of dorsal clock neurons (DN1), raising the possibility of a direct modulatory effect exerted by the circadian system [33]. Indeed, natural variants of the *timeless* clock gene in *D. melanogaster*, namely the *s-tim* and *ls-tim* allelic variants, are known to have a dramatic effect on the inducibility of reproductive dormancy [37,38].

In our study, we primarily focused on neuronal clusters that, based on their axonal projections to the dorsal brain (dorsal protocerebrum), could play an intermediary role in conveying dormancy-inducing signals towards the IPCs. Neurites of the small ventral lateral neurons (s-LN$_v$s) project to the dorsal protocerebrum, where they rhythmically release the circadian neuromodulator PIGMENT DISPERSING FACTOR (PDF) [39]. PDF is also expressed in the large ventral lateral neurons (l-LN$_v$s), and in two groups of non-clock cells, a developmentally transient neuronal cluster in the Tritocerebrum (designated as PDF-Tri), and a small number of neurons in the eighth abdominal neuromere of the ventral ganglion (designated as PDFAb neurons) [40]. PDF is a key coordinator of pacemaker interactions and behavioral rhythms [41–43], of sleep and arousal [44,45] and of sexual behavior [46]. PDF may also be involved in diapause regulation in the blow fly *Protophormia terraenovae* [47], the mosquito *Culex pipiens* [48], and the bean bug *Riptortus pedestris* [49]. However, its effects appear to be contradictory and the mechanisms through which PDF acts on diapause are unclear.

Short Neuropeptide F (sNPF) has been implicated in the modulation of diapause in the Colorado potato beetle [50] and has been shown to stimulate ovarian development in the locust [51,52]. In *Drosophila* sNPF increases food intake and body size [53] and enhances growth [54]. This peptide is broadly produced in the *Drosophila* nervous system [53,55], including the s-LN$_v$s [56]. A small set of bilaterally symmetric neurons in the *Pars lateralis* (PL), defined as dorsal-lateral peptidergic neurons (DLPs), also express sNPF. DLPs have axon terminations in the proximity of the IPCs, and co-express the multi-functional neuropeptide Corazonin (Crz) [57], which has also been proposed as a diapause regulating peptide in the hawkmoth *Manduca sexta* [58].

The G protein-coupled receptors for PDF, sNPF, and Crz (PDFR, sNPFR1, and CrzR, respectively) have already been characterized and extensively studied in *Drosophila* [57,59–67]. Interestingly, sNPFR1 and CrzR have been found to influence the activity of the IPCs [53,54,57,68]. However, to date no studies have reported PDF signaling to the IPCs.

In the present study, we demonstrate that PDF and sNPF produced by PDF-positive (PDF^{+}) neurons, reduce the induction of dormancy in *Drosophila*, mainly through a direct effect on the IPCs. Conversely, the Corazonin-expressing DLP neurons do not seem to be involved. Using live imaging, we show that the IPCs respond to both PDF and sNPF peptides with increasing levels of cAMP and to sNPF additionally with increasing Ca^{2+} levels suggesting that PDF and sNPF positively modulate IPCs activity and thereby inhibit gonadal arrest.

Results

Genetic manipulations of PDF^{+} neurons alter dormancy levels

To examine whether the PDF-expressing neurons have a role in the regulation of reproductive arrest, we used a *Pdf*-Gal4 driver to target gene expression specifically in PDF^{+} neurons including both s- and l-LN$_v$s [39,41]. First, a bacterial depolarization-activated sodium channel (Na^{+}ChBac) was expressed in these neurons (*Pdf>Na^{+}ChBac*). Such manipulation will enhance the release of neurotransmitters and neuropeptides, including PDF and sNPF [69]. *Pdf>Na^{+}ChBac* flies showed significantly lower levels of dormancy compared to controls (p<0.001; Fig 1A). Importantly, Na^{+}ChBac expressing and control flies shared the same *timeless* (*tim*) background, as *tim* alleles (*s*- and *ls-tim*) affect the overall level of reproductive arrest (S1 Table) [37]. We also overexpressed PDF in the same subset of cells (*Pdf>Pdf*), which again resulted in a significant decrease in the incidence of dormancy compared to controls (p<0.001; Fig 1A).

In addition to PDF, the s-LN$_v$s co-express the neuropeptide sNPF. Since sNPF is widely present in the nervous system [53,55], we started by overexpressing this neuropeptide with a
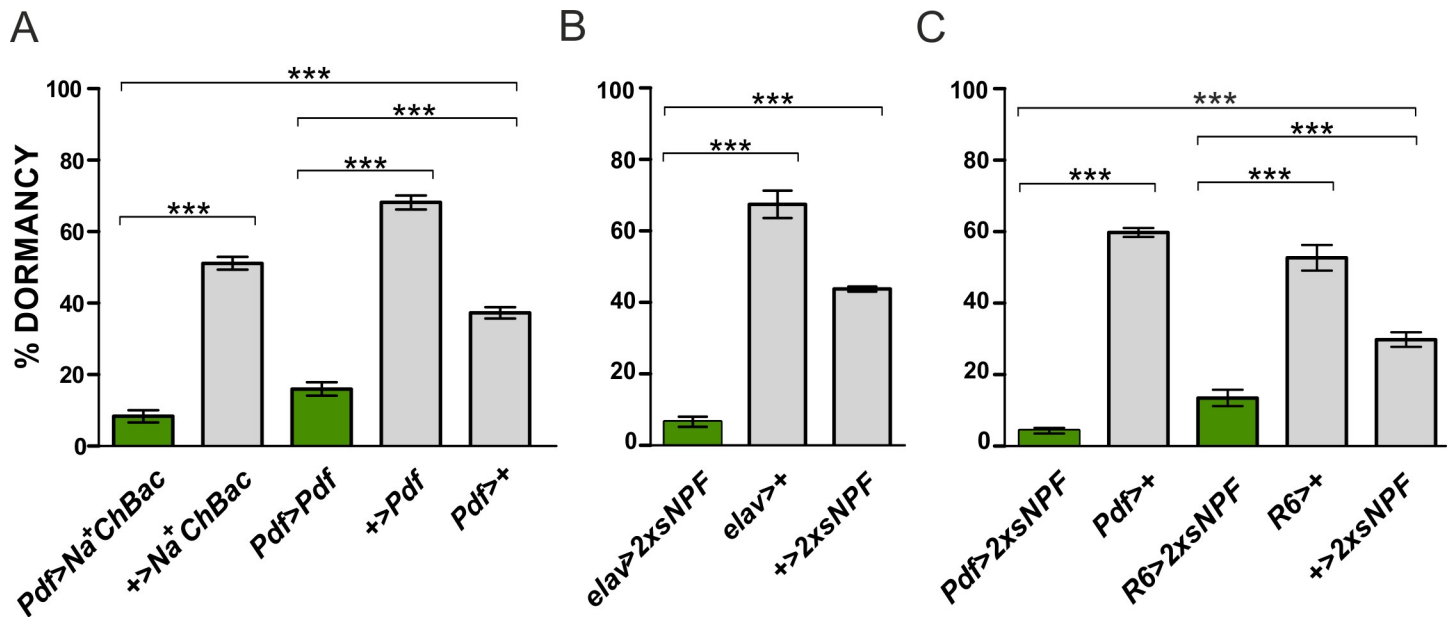
Fig 1. Enhanced activity of PDF-expressing neurons reduces dormancy levels. (A) Hypersensitization of PDF$^+$ neurons (*Pdf>Na$^+$ChBac*) and overexpression of PDF (*Pdf>Pdf*) both result in a significant reduction of reproductive arrest. (B) Pan-neuronal overexpression of sNPF (*elav>2xsNPF*) leads to a significant decrease in the proportion of arrested females. (C) Overexpression of sNPF in the PDF-expressing neurons (*Pdf>2xsNPF*) and in the small ventrolateral neurons (*R6>2xsNPF*) triggers females to exit from dormancy. Numbers within bars refer to the number of dissected females considered in the dormancy assays. Data are presented as mean ± SEM. ANOVA on arcsine transformations, followed by *post-hoc* Tukey HSD test. ***p<0.001, n.s. not significant.

pan-neuronal driver. This manipulation (*elav>2xsNPF*) produced a very significant reduction in dormancy in the experimental flies compared to the controls (p<0.001; Fig 1B). Considering that both the *elav*-Gal4 and the UAS-*2xsNPF* lines carry the *ls-tim* allele (S1 Table), which is known to promote ovarian quiescence [37], the antagonistic effect of sNPF is quite dramatic. We then narrowed the overexpression of the neuropeptide specifically to the PDF$^+$ neurons (*Pdf>2xsNPF*) and detected a similar and highly significant reduction of ovarian arrest in the experimental flies compared to the controls (p<0.001; Fig 1C). These results suggest that the Pdf-expressing tissues (the s-LN$_v$s, l-LN$_v$s, the PDF-Tri and the PDF-Ab) are making the major contribution to the inhibition of dormancy. To test the importance of the s-LN$_v$s we used the *R6*-Gal4 driver [70] which is active in the s-LN$_v$s and in some other neurons but not in the remaining PDF$^+$ cells [71]. Again, *R6>2xsNPF* flies showed significantly reduced dormancy when compared to controls (p<0.001; Fig 1C). Thus, we conclude that sNPF, likely released from the s-LN$_v$s, is involved in the negative regulation of gonadal arrest.

We then considered the opposite manipulation, namely reduced neuronal excitability, which ultimately results in reduced release of neuropeptides. Neuronal overexpression of the potassium channel Ork increases potassium efflux and causes membrane hyperpolarization, thereby preventing the firing of action potentials [72]. *Pdf>Ork* flies showed higher levels of ovarian arrest compared to controls (p<0.001; Fig 2A). Furthermore, genetically ablating the PDF$^+$ neurons by overexpressing the pro-apoptotic protein hid (head involution defective), *Pdf>hid*), also caused a larger proportion of females to undergo dormancy compared to controls (p<0.001; Fig 2B).

As the PDF neurons co-express more than just PDF we also examined whether the *Pdf^{01}* null mutation would alter dormancy levels at two photoperiods, LD8:16 and LD16:8. The experiment was performed on the *ls-tim* background. Fig 2C reveals that there is a significant genotype effect (p = 1.3 x 10^{-4}) with *Pdf^{01}* mutants showing significantly elevated levels of
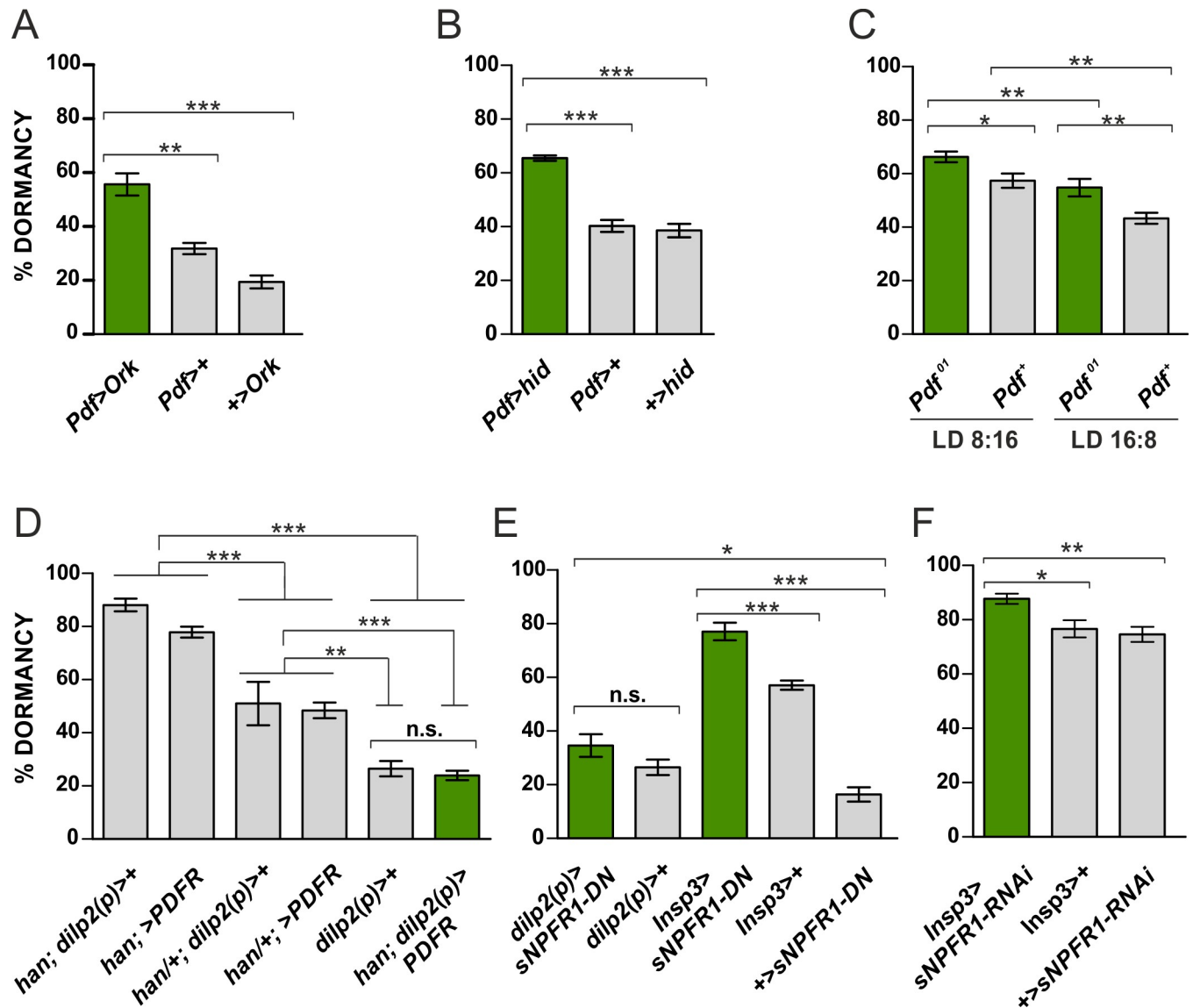
Fig 2. Inhibited neuronal activity of PDF⁺ neurons and impairment of sNPF signaling in the IPCs increase dormancylevels. (A) Expression of the potassium channel Ork (*Pdf>Ork*) enhances incidence of gonadal arrest in the experimental flies compared to control females. (B) Genetic ablation of PDF-expressing neurons (*Pdf>hid*) provokes a higher proportion of females entering dormancy compared to controls. (C) *Pdf⁰¹* mutant females show enhanced ovarian quiescence levels compared to a congenic wild-type control at both summer and winter photoperiods (see text). (D) PDFR overexpression in IPCs in a *han/han* mutant background significant reduces dormancy compared to homozygous and heterozygous *han/+* controls, but not compared to the wild-type control *dilp2 (p)>+*, which also appears as one of the controls in Fig 2E. (E) Overexpression of a dominant negative form of sNPFR1 (UAS-*sNPFR1-DN*) in the IPCs under the control of an early and a later-expressed IPC driver (*dilp2(p)*-Gal4 and *Insp3*-Gal4, respectively) increases dormancy levels. (F) Downregulation of *sNPFR1* with RNAi using the *Insp3*-Gal4 driver significantly enhances reproductive arrest compared to controls. Numbers within bars indicate the number of dissected females considered in the dormancy assays. Data are presented as mean ± SEM. ANOVA on arcsine transformations, followed by *post-hoc* tests. ***p<0.001, **p<0.01, *p<0.05, n.s. not significant.

ovarian quiescence plus a significant photoperiodic effect (p = 6 x 10⁻⁶), with no significant interaction, so the enhancement in dormancy occurs at both photoperiods equally. We also examined the effects of overexpressing the PDF receptor (PDFR) in the IPC cells using *dilp2 (p)*-Gal4 [21,73] in a homozygous receptor mutant *han* background. This was compared to parental controls (*dilp2(p)*-Gal4 and UAS-*PDFR*) that were both homozygous and heterozygous for *han*, as well as the *dilp2(p)>+* wild-type control. All six genotypes were placed on the

s-tim background. Fig 2D reveals that overexpression of *PDFR* causes a highly significant reduction of dormancy (p<0.001) compared to all the corresponding *han/han* and *han/+* controls, but is not significantly different from the *dilp2(p)>+* wild-type. Consequently, we appeared to have rescued the mutant phenotype in this genetic background. The heterozygous *han/+* background controls also show a highly significant reduction of dormancy compared to their corresponding homozygous mutant controls (both p<0.001) and the *dilp2(p)>+* wild type (p<0.01), further underscoring the dosage effect of PDFR on the phenotype. All of these experiments are consistent with the view that the s-LN$_v$s modulate dormancy levels via the neuropeptides PDF and sNPF. However, since *Pdf*-Gal4 is also expressed in the non-circadian PDF-Tri and PDF-Ab neurons [39,41], an influence of the latter cannot be excluded.

sNPFR1 signaling in the IPCs modulates reproductive arrest

The IPCs express sNPFR1 [54,57,68]; its activation by sNPF stimulates organismal growth by promoting the transcription of insulin-like peptides genes [54]. To investigate whether sNPFR1 signaling in the IPCs modulates ovarian arrest we expressed a dominant negative form of the receptor (UAS-*sNPFR1-DN*) under the control of two IPCs-specific drivers: *dilp2 (p)*-Gal4 and *InsP3*-Gal4 [21,73]. The former drives gene expression from the 2nd larval instar, the latter becomes active mainly after larval development [73].

Inhibition of sNFR1 from early larval stages (*dilp2(p)>sNPFR1-DN*) increased only marginally the proportion of dormancy (Fig 2E). However, when the receptor was repressed later in development (*InsP3>sNPFR1-DN*), a significantly higher proportion of flies showed gonadal arrest compared to controls (p<0.001; Fig 2E). Both drivers are specific for the 14 IPCs in the brain [21,73], so we speculate that different degrees of dormancy might reflect differences in the strength of the drivers or compensatory phenomena that occur early in development. We also used the *InsP3* driver to knockdown *sNPFR1*. We observed a significant increase in gonadal arrest in *InsP3> SNPFR1 RNAi* compared to the Gal4 (p = 0.017) and UAS controls (p = 0.006) (Fig 2F). These results are consistent with our previous observations regarding the antagonist nature of sNPF on this phenotype (Fig 1B and 1C), and also suggest a role for sNPF signaling in the IPCs in the regulation of reproductive arrest.

No evidence for the involvement of the DLPs in the regulation of dormancy

The dorsal-lateral peptidergic neurons (DLPs) are 6–7 bilaterally symmetric neurons in the *Pars Lateralis* (PL) whose axons ends in the proximity of the IPCs [57]. The DLPs produce the neuropeptides Corazonin (Crz) and sNPF through which they modulate the activity of the IPCs, as the latter express the relevant receptors, CrzR (Corazonin Receptor) and sNPFR [57]. The DLPs affect survival, stress resistance and levels of circulating carbohydrates and lipids [57,74]. Since diapause is associated with marked changes of these parameters, we questioned whether the DLPs are involved in the regulation of this seasonal response. We used two DLP-specific *Crz*-Gal4 driver lines, *Crz$_1$*-Gal4 and *Crz$_2$*-Gal4, to overexpress Na$^+$ChBac and sNPF, respectively. Both *Crz$_1$>Na$^+$ChBac* and *Crz$_2$>2xsNPF* flies showed a reduction in the proportion of females undergoing gonadal dormancy (p<0.001) compared to one of the parental controls but not the other (S1 Fig). Therefore, although we cannot totally exclude an effect of the DLPs on ovarian arrest we can conclude that their involvement, if any, is not as robust as that observed for the PDF$^+$ neurons.

Terminals of the s-LN$_v$s overlap with fine processes from the IPCs

Next, we asked whether the dorsal terminals of the s-LN$_v$s in the dorsal vicinity might be close enough to the IPCs to enable such sNPF and PDF signaling. By performing ICC with anti-

DILP2 and anti-PDF we could not see direct contacts overlapping between the s-LN$_v$s and the IPCs (Fig 3A). However, when we expressed GFP in the IPCs (*dilp2(p)>GFP*), we observed that the dorsal projections of the s-LN$_v$s are in close proximity to fine processes originating from the IPCs (Fig 3B). To test whether these fine processes are dendrites, we expressed the dendritic marker DenMark in the IPCs (*dilp2(p)>DenMark*) [75]. We found prominent labeling in the IPC processes, indicating that they are of dendritic origin (Fig 3C and 3D). This explains why we could not see them by anti-DILP2 labeling.

IPCs respond to bath-applied PDF and sNPF

The IPCs are neurosecretory cells that are crucial for initiating seasonal responses [13,17,19,20]. Since we have shown that PDF and sNPF have a modulatory effect on diapause (Fig 1), and that PDF$^+$ and sNPF$^+$ neurons appear to contact the IPCs (Fig 3B)[57], we asked whether the IPCs can respond directly to these neuropeptides. The PDF receptor signals primarily via cAMP [59,61,76], whereas the signaling cascade following activation of the receptor for sNPF uses cAMP, at least in part [77–79]. Thus, we expressed a genetically encoded fluorescence resonance energy transfer (FRET) based cAMP sensor in the IPCs (*dilp2(p)>Epac1-camps*) to monitor real-time cAMP levels [62]. A similar experimental design had previously been adopted with success to investigate the presence of the PDF receptor in clock neurons [62].

We bath-applied 10 **μ**M of synthetic PDF to acutely dissected fly brains. This resulted in a slow rise in the intracellular amount of cAMP, measured as the average FRET signal between 100 and 1000 s after the application of the neuropeptide (light-blue curve and bar; Fig 4A and 4B). cAMP FRET signals were 10% *ca.* higher (100–1000 s; p<0.001) compared to the negative (modified minimal hemolymph-like solution, HL3, light-grey curve and bar; Fig 4A and 4B) control. A similar increment was also observed after presenting PDF together with the sodium channel blocker tetrodotoxin (TTX, dark-blue curve and bar, 100–1000 s; p<0.001; Fig 4A and 4B). The latter prevents neuronal communication, suggesting that PDF activates the IPCs directly. However, the short-term (100-200s) response to PDF was unchanged compared to the negative control, either with or without TTX (Fig 4C and 4D).

Similar observations were made upon the application of 10 **μ**M synthetic sNPF. This resulted in a slow but significant cAMP increase in the IPCs either in the absence (yellow curve and bar, 100–1000 s; p<0.001) or in the presence (orange curve and bar, 100–1000 s; p<0.001) of TTX, reflecting a direct activation of the IPCs by sNPF (Fig 4E and 4F). Moreover, as we saw for PDF, the short-term responses to sNPF did not differ from the negative control (Fig 4G and 4H).

However, when we applied sNPF and PDF together (sNPF+PDF), at a concentration of 10 **μ**M for each peptide, we recorded an increase in cAMP FRET signal, reaching a level ~15% higher than that for the negative control (red, 100–1000 s; p<0.001; Fig 5A and 5B). Moreover, the short-term response was particularly distinctive compared to the applications of single peptides, revealing a ~8% increase in cAMP FRET signals (red curve and bar; 100–200 s; p<0.01; Fig 5C and 5D). We repeated the experiment but halving the concentration of each peptide to 5 **μ**M (sNPF$_{1/2}$+PDF$_{1/2}$). This also resulted in a significant increase in cAMP (pink curve and bar, 100–1000 s; p<0.05; Fig 5A and 5B). However, we noticed that following an initial increase, after 400 s the concentration of cAMP slowly declined (pink curve and bar; Fig 5A). Focusing on the short-term response, the co-application of (sNPF$_{1/2}$+PDF$_{1/2}$) resulted in higher cAMP FRET signals compared to the bath treatment with single peptides; however, the difference was statistically significant only with regard to PDF (100-200s; p<0.01; Fig 5C and 5D).
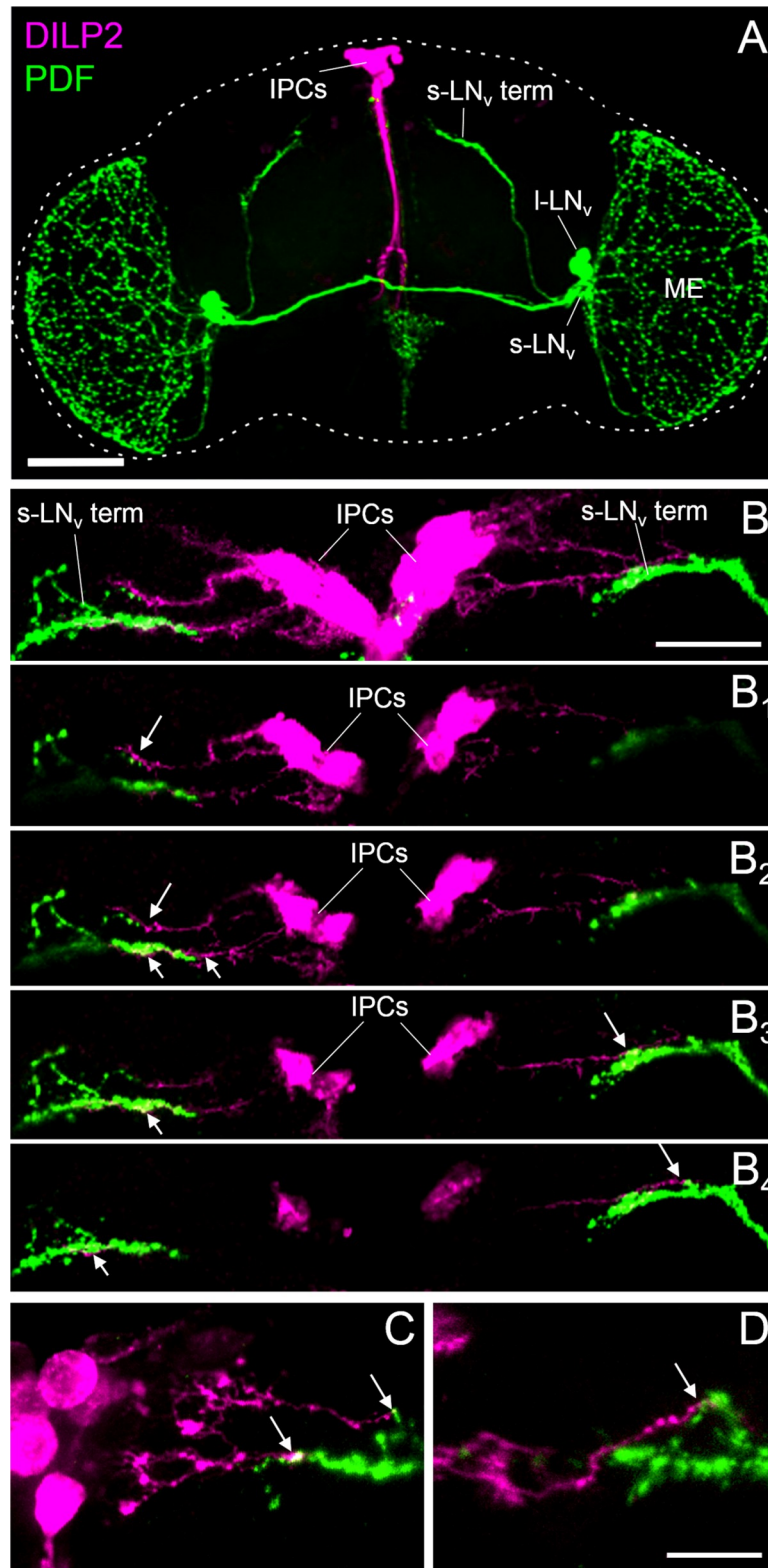
Fig 3. The terminals of the PDF positive s-LN$_v$s overlap with dendrites of the insulin producing cells (IPCs). (A) Representative confocal image (overlay of Z-stacks through the entire brain) of a *Hu-S* fly brain double-stained with antibodies against PDF (green) and DILP2 (magenta). The brain is outlined by a dashed line. Me = medulla. Scale bar = 100 μm. (B) Representative confocal image of the dorsal part of *dilp2(p)>GFP* brains double stained with

antibodies against PDF (green) and GFP (magenta) (overlay of 10 Z-stacks). Processes of the insulin producing cells (IPCs) overlap with the terminals of the small ventrolateral neurons (s-LN$_v$ term) as can be seen in single confocal stacks of 2 μm thickness (B_1-B_4). Every second single stack of the posterior part of (B) is shown from anterior to posterior. White arrows indicate close proximity between IPCs and s-LN$_v$ terminals. Scale bar = 20 μm. (C-D) Labeling of the IPCs with the dendritic marker DenMark [75] (*dilp2(p)>DenMark*) indicate that the IPC fibers contacting the s-LN$_v$ terminals are of dendritic origin. Representative confocal images of two different brains are shown. Scale bar 10 μm.

We also tested (sNPF+PDF+TTX) and found an increase of ~13% in the amount of cAMP FRET signal compared to the negative control (magenta curve and bar, 100–1000 s; p<0.001; Fig 5E and 5F). This response was not statistically different from single peptide applications in the presence of TTX although in the interval 300–600 s the levels of cAMP for (sNPF+PDF +TTX) were higher (Fig 5E and 5F). Interestingly, although there were no differences in cAMP levels when comparing the application of sNPF+PDF with or without TTX in the
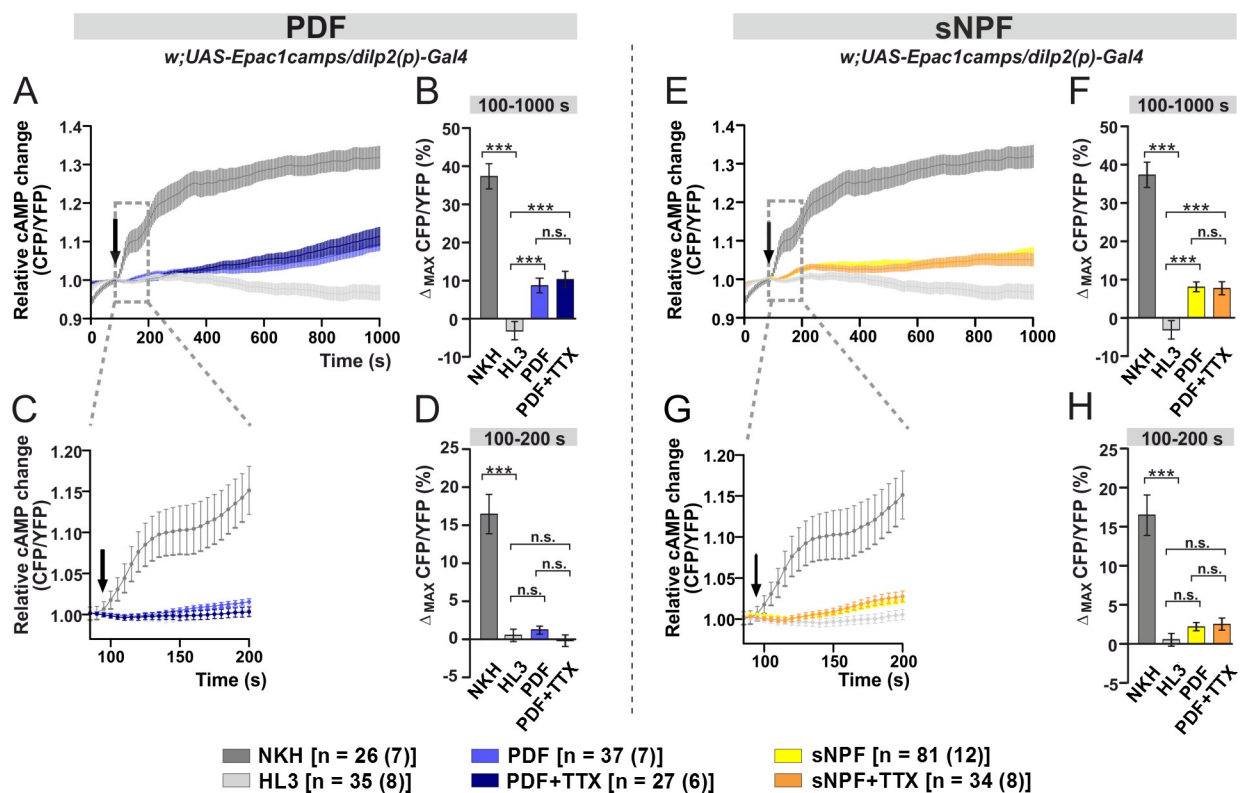
Fig 4. Bath-applied PDF and sNPF induce cAMP increases in the IPCs. Live optical imaging in flies expressing a cAMP sensor in their IPCs (*dilp2(p)>Epac1camps*). Average inverse FRET traces (CFP/YFP) in IPCs reflecting intracellular changes in cAMP levels. Substances were bath-applied to freshly dissected fly brains at 100 s (indicated by black arrow). Application of 10^{-5} M adenylate cyclase activator NKH477 (NKH, dark gray) induced a robust increase in cAMP, indicating that the general procedure was working. As a negative control, hemolymph-like saline (HL3) was applied. (A) Bath-applied PDF (10^{-5} M) evokes cAMP increases in the IPCs (light blue), suggesting a possible functional connection between PDF$^+$ cells and IPCs. Similar increase was observed when PDF was applied in the presence of 2μM sodium channel blocker tetrodotoxin (TTX; dark blue), indicating a direct connection. (B) Maximum inverse FRET changes quantified for each individual neuron and averaged for each pharmacological treatment between 100–1000 s. (C) A close-up of the immediate changes in cAMP levels occurring from the application point until 200 s. No significant changes can be observed when PDF or PDF+TTX were applied. (D) Maximum inverse FRET changes from 100–200 s. (E) Bath-applied sNPF (10^{-5} M) generates cAMP rises in the IPCs (yellow). Similar increase occurs in the presence of TTX (orange), thus suggesting a direct connection. (F) Maximum inverse FRET changes between 100–1000 s. (G) Magnification of the immediate changes between 100–200 s. (H) Maximum inverse FRET changes between 100–200 s. The legend shows the color code of the different treatments and the number of neurons in the dissected brains (in parentheses) considered in this analysis. Data are shown as mean ± SEM. Kruskal-Wallis test followed by Bonferroni-corrected Wilcoxon pairwise-comparisons. ***p<0.001, **p<0.01, *p<0.05, n.s. not significant.
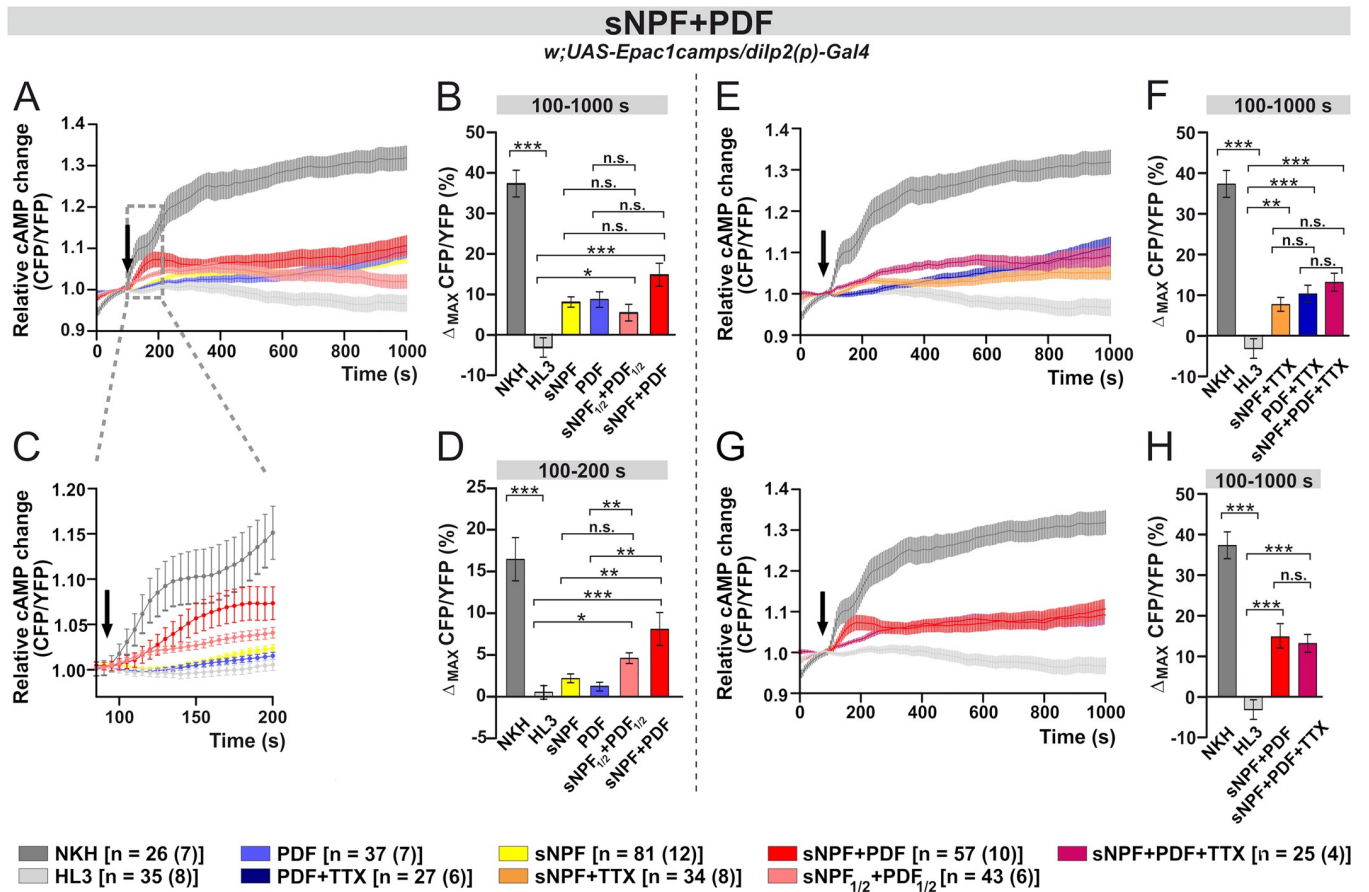
Fig 5. The co-application of PDF and sNPF increase the cAMP response. (A) Co-application of sNPF and PDF evokes large cAMP increases in the IPCs (red), which remain significant even when concentrations of peptides are halved (rose). (B) Maximum inverse FRET between 100–1000 s. (C, D) Immediate cAMP responses (100–200 s) reveal a large, rapid increase due to the sNPF+PDF co-application. (E) Co-application of sNPF and PDF induces cAMP increases in the IPCs also in the presence of TTX (magenta), and this response seems to be larger in the time interval of 200–600 s than the effect triggered by the application of the single peptides with TTX. (F) Maximum inverse FRET changes from 100–1000 s. (G) The effect of the sNPF+PDF co-application seems to be, at least partially, due to a direct activation of the IPCs. The initial increase is apparently reduced when TTX is present (magenta). (H) Maximum inverse FRET changes from 100–1000 s. The legend shows the color code of the different treatments and the number of neurons in the dissected brains (in parentheses) considered in this analysis. Data are shown as mean ± SEM. Labeling as in Fig 4.

https://doi.org/10.1371/journal.pgen.1008158.g005

interval 100–1000 s, the distinctive short term response disappeared in the presence of TTX (Fig 5G and 5H). This suggests that the short-term response of the IPCs to the combined application of (sNPF+PDF) is indirectly mediated by other cells.

We assessed whether the larger increase in cAMP levels induced in the IPCs by the co-application of sNPF+PDF is a specific response. We co-applied sNPF with the following neuropeptides: SDNFMRFamide (SDNFMRFa), adipokinetic hormone (AKH), *Drosophila* tachykinin (DTK) and allatostatin-C (Ast-C). AKH and DTK were chosen because they are known regulators of IPC activity [21,73,80,81]. When sNPF was co-applied with SDNFMRFa, AKH or DTK, the levels of cAMP were significantly reduced compared to the sNPF+PDF co-application ($p<0.05$, $p<0.01$, $p<0.05$, respectively) and were indistinguishable from the negative control (Fig 6). Conversely, the co-application of sNPF+Ast-C resulted in a significant increase in the amount of cAMP but the addition of Ast-C alone was sufficient to evoke similar cAMP responses in the IPCs (Fig 6). To our knowledge, no data are available on the distribution of the Ast-C receptor in *Drosophila*, and no link between IPCs and Ast-C has been reported previously. In summary, our data show that the strong and rapid responses of the IPCs we

Fig 6. Co-application of sNPF with other *Drosophila* peptides suggests that sNPF and PDF may have a unique interaction. (A) Average inverse FRET traces (CFP/YFP) of IPCs reflecting intracellular cAMP changes. 10^{-5} M synthetic sNPF was co-applied with PDF, SDNFMRFa, AKH (adipokinetic hormone), DTK (Drosophila tachykinin), Ast-C (Allatostatin-C) /10^{-5}M for each/ or 10^{-5} M Ast-C was added alone. The black arrow indicates the application point of the different substance. NKH: adenylate cyclase activator, used as positive control. HL3: hemolymph-like saline, used as negative control. (HL3) (B) Maximum inverse FRET changes quantified for each individual neuron and averaged for each treatment from 100 s until 1000 s. Statistical comparison revealed that co-application of sNPF with SDNFMRFa, AKH, and DTK resulted in a significant decrease of cAMP levels compared to the sNPF+PDF co-application. sNPF+Ast-C led to a significant increase in

the level of cAMP, however similar change was observed in the case of Ast-C application alone. (C) A close up of the immediate cAMP level changes occurring from the application point until 200 s. (D) Maximum inverse FRET from 100 s until 200 s. The legend indicates the color code of the different treatments and the number of neurons in the dissected brains (in parentheses) considered in this analysis. ***$p < 0.001$, **$p < 0.01$, *$p < 0.05$, n.s. not significant.

observed are unique to the co-application of PDF and sNPF. In particular, they are not caused either by the combination of other peptides or by receptor cross-activation due to high peptide doses applied.

To verify whether the responses to PDF were mediated by its receptor, we carried out the treatment in the PDFR-null (*han*) [59] background (*han; dilp2(p)>Epac1camps*). The application of PDF in the mutant no longer evoked an increase of cAMP (light-blue; 100–1000 s; Fig 7A–7D), and surprisingly, neither did sNPF (yellow curve and bar; 100–1000 s; Fig 7A–7D). The rapid increase in cAMP levels induced by the co-application of sNPF+PDF was also obliterated in the mutant (red curve and bar; 100–200 s; Fig 7C and 7D). To test whether sNPF acts via PDFR, we rescued PDFR expression in the IPCs in the *han* mutant background (*han; dilp2 (p)>PDFR; Epac1camps*). In these flies, IPCs strongly responded to PDF, but not to sNPF. It is therefore unlikely that sNPF signals via PDFR (Fig 7E–7H). We observed a slight increase in cAMP ~400s after sNPF application, but this was not significantly different from the negative controls (yellow curve and bar; 100–1000 s; Fig 7E and 7F). The fast response to sNPF was completely absent (yellow curve and bar; 100–200 s; Fig 7G and 7H). This shows that the absence of the response to sNPF in the *han* mutant cannot be directly attributed to the loss of PDFR.

sNPF but not PDF increases Ca^{2+} levels in the IPCs

In several cell types PDF signals primarily through cAMP rather than calcium [59,61,76]. Here we tested whether PDF or sNPF affect the level of intracellular Ca^{2+} in the IPCs by expressing the genetically encoded Ca^{2+} sensor GCaMP3.0 (*dilp2(p)>GCaMP3.0*) [82] Incubating PDF with freshly dissected brains did not produce change in Ca^{2+} levels, which were indistinguishable from the negative control (Fig 8). However, the bath application of sNPF induced a small but significant increase in the Ca^{2+} signal (100-200s, 3.4 ± 2.8%, $p < 0.05$). This was still detectable in the presence of TTX (100-200s, 5.4 ± 3.5%, $p < 0.05$), suggesting that this response is not mediated by interneurons but is due to the direct activation of the IPCs by sNPF (Fig 8).

Discussion

Genetic manipulations of PDF-expressing neurons modulate dormancy

We have constitutively activated the PDF$^+$ neurons with Na$^+$ChBac [69] and observed a significant reduction in levels of gonadal arrest (Fig 1A). Since this treatment increases membrane excitability, it likely increases release of both PDF and sNPF, whose overexpression also led to a significant reduction in dormancy (Fig 1B and 1C). Manipulations with opposite effect, namely reduction of membrane excitability of the PDF$^+$ neurons through overexpression of the K$^+$ channel Ork [72] or induction of cell death by overexpression of the pro-apoptotic gene *hid*, resulted in an enhanced dormancy response (Fig 2A and 2B). Furthermore, the *Pdf^0* mutant showed a significantly elevated response compared to controls and overexpressing *PDFR* in the IPCs significantly reduced gonadal arrest on both heterozygous and homozygous mutant *han* backgrounds to wild-type levels. These results consistently support a model where PDF and SNF act to antagonise dormancy, possibly by enhancing dILP expression. When we expressed a dominant negative form of the sNPF receptor in the IPCs, or downregulated the
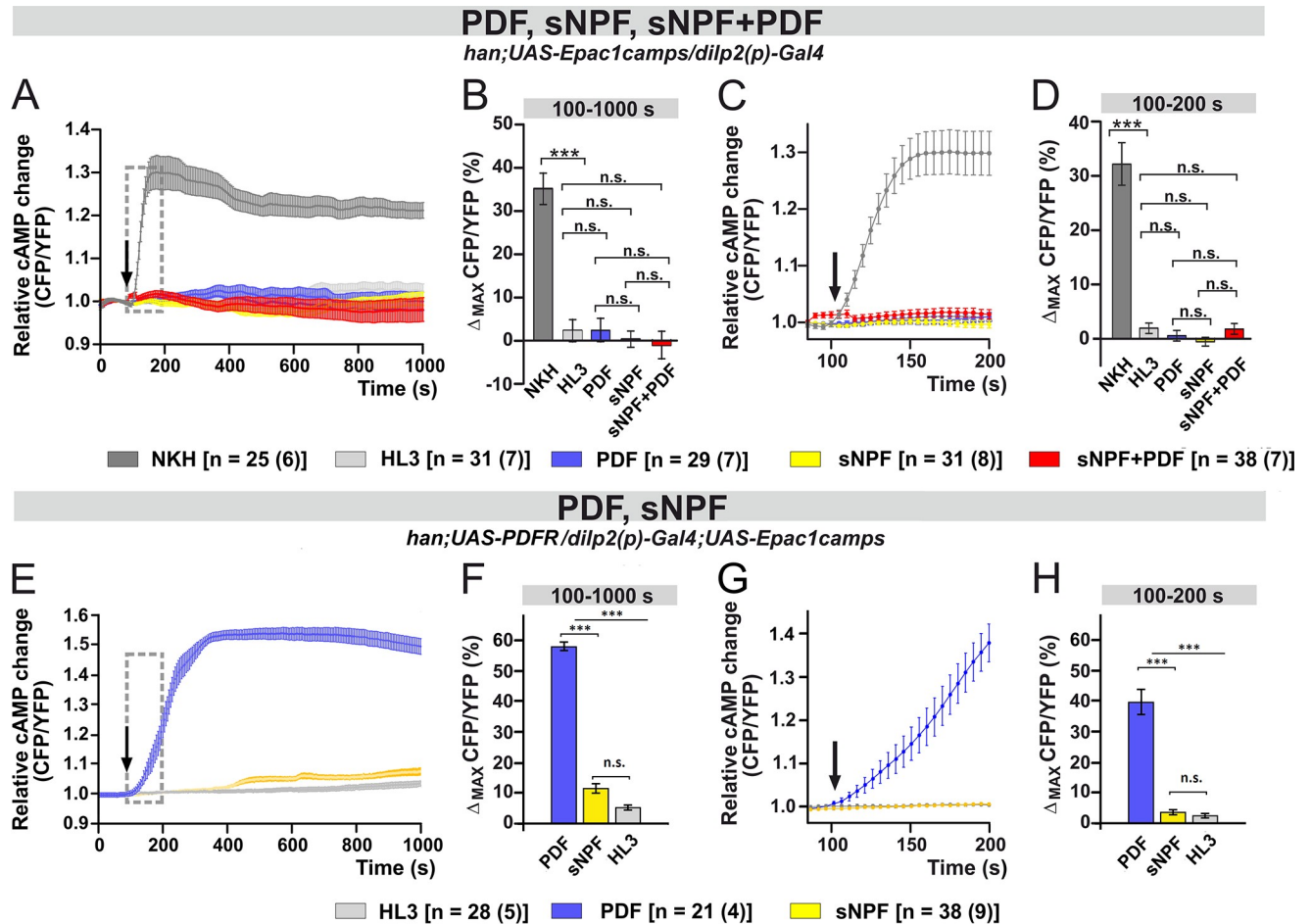
Fig 7. The responses of the IPCs to PDF and sNPF are absent in the PDF receptor mutant *han*, but only the response to PDF is mediated by the PDF receptor. (A-D) Live imaging in *han* mutants expressing a cAMP sensor in their IPCs (*han; dilp2(p)>Epac1camps*). In the mutant background, the effects of both neuropeptides are abolished. (A-B) Maximum inverse FRET changes from 100–1000 s. Short-term responses are all abrogated in *han* flies. (C-D) Maximum inverse FRET changes from 100–200 s. (E-H) Live imaging in *han* mutants with the PDF receptor rescued in the IPCs. The expression of *han* in the IPCs induces very strong responses to PDF but not to sNPF (E-F) Maximum inverse FRET changes from 100–1000 s. (G-H) Maximum inverse FRET changes from 100–200 s. Labeling as in Fig 4.

https://doi.org/10.1371/journal.pgen.1008158.g007

receptor with RNAi, higher dormancy induction was observed especially when using a driver that is active later in development (Fig 2E and 2F). Numerous sNPF-expressing neurons can potentially target the IPCs, including the PDF+ sLN$_v$s and the DLPs. However, the manipulations of the DLPs did not affect reproductive quiescence (S1 Fig).

One puzzling aspect of the results is that they appear, at least superficially, to contradict a recent study in which *Pdf*[01] females showed relatively low levels of dormancy and did not reveal a photoperiodic effect [83]. The LD cycles used in these experiment were LD16:8 versus LD10:14 so not as extreme as ours and this might have had a damping effect on any photoperiodicity. Furthermore, the low dormancy levels of the mutant females suggested that the mutation might have been on the *s-tim* background. A congenic wild-type was not compared to the mutant, so it is difficult to predict whether such a control would have had lower levels of reproductive arrest which would be consistent with our findings. In addition, the further stress of starvation was incorporated into the experimental paradigm. It would therefore be of interest to examine whether our results, which suggest that the neuropeptides released by clock cells
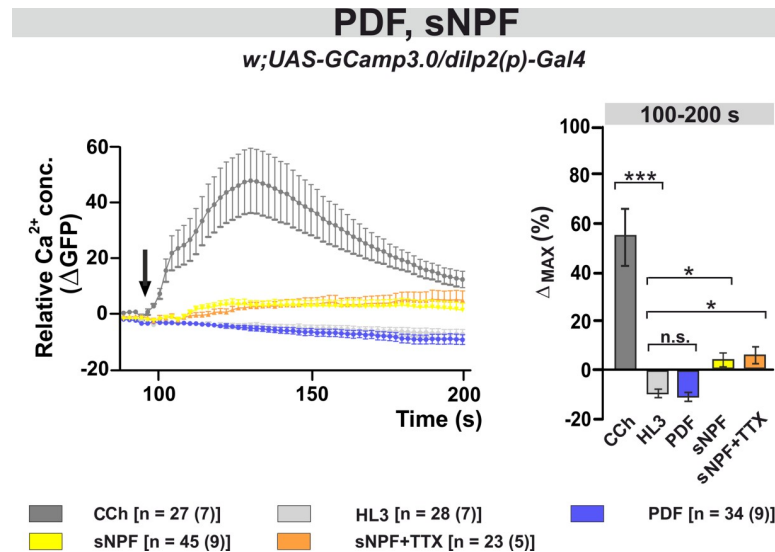
Fig 8. The neuropeptide sNPF induces a small increase in the intracellular Ca²⁺ level, while PDF has no effect. Left panel: Average changes in GFP fluorescence of IPCs reflecting intracellular changes in Ca²⁺ levels. Substances were bath-applied to freshly dissected fly brains at ~100 s (indicated by a black arrow). The cholinergic agonist carbamylcholine (1 mM CCh) was used as positive control, which induced a robust increase in Ca²⁺, indicating that the general procedure was working. As a negative control, hemolymph-like saline (HL3) was applied. Application of 10–5 M synthetic PDF peptide did not alter Ca²⁺ levels, while 10–5 M sNPF induced a small but significant increase in Ca²⁺ levels. This calcium response seems to be due to direct activation of the IPCs, since it was not blocked in the presence of the sodium channel blocker TTX (2μM). Right panel: Maximum Ca²⁺ changes (%) for each individual neuron were calculated and averaged for each pharmacological treatment from 100 s until 200 s. Statistical comparison revealed significant increases in Ca²⁺ levels compared to the negative control (HL3) for CCh, sNPF and sNPF+TTX, while PDF had no effect. Data are presented as mean ± SEM. The color code of the different treatments and the number of neurons [n] and dissected brains (n) considered in this analysis are shown below the panels. Kruskal-Wallis test followed by Bonferroni-corrected Wilcoxon pairwise-comparisons. ***p<0.001, *p<0.05, n.s. not significant.

antagonise reproductive quiescence, can be generalized under a variety of different unfavourable environmental conditions.

The IPCs respond to PDF and sNPF

Using a whole brain *ex-vivo* preparation, we observed that the IPCs responded to bath-applications of sNPF and PDF with increasing cAMP levels. The responses persisted when synaptic connections with the rest of the brain were inhibited by TTX, suggesting a direct effect on the IPCs of these neuropeptides (Fig 4A–4H). Expression of sNPFR1 in the IPCs had already been described [53,54,57,68]. Interestingly, sNPFR1 couple to more than one Gα-protein subtype, since both excitatory (through $G_s\alpha$ [77,78]) and inhibitory effects (through $G_o\alpha$ [79]) on cAMP levels have been documented. In addition, sNPF can signal by suppressing Ca²⁺ in some circadian clock clusters [42] and peptidergic PTTH neurons [84]. Here, we found that sNPF increased Ca²⁺ levels in the IPCs showing that it can also have activating Ca²⁺ effects. Similar multiple G-protein coupling has also been reported for the neurokinin-1 and -2 receptors [85,86], as well as for the glucagon receptor in human atrial membranes [87].

The expression of the PDFR in the IPCs is less well-characterized. A previous study using fluorescent *in situ* hybridization reported prominent *PDFR* expression in the PI. However, it did not identify the *PDFR* positive cells [60]. Moreover, another study suggested that the cAMP responses evoked in the IPCs by PDF are not as robust as those registered in clock neurons [62]. Possibly, lower ligand efficacy might simply reflect less PDFR in these cells. The

strong cAMP responses we observed after driving PDFR in *han* mutants under control of *dilp2(p)*-Gal4 supports this conclusion (Fig 6E–6H). On the other hand, there are 14 IPCs in the PI which show heterogeneous protein and neuropeptide composition [29,88], and rhythmic electrophysiological parameters [33]. Thus, it is possible that, like the s-LN$_v$s [89], the responsiveness of the IPCs to PDF is also influenced by time of day. In any case, here we found significant cAMP increasing effects of PDF on the IPCs.

When we applied sNPF and PDF together, the short-term (100–200 s) response of the IPCs to the combined peptides was greater than the sum of their separate activities, pointing to a synergistic effect between the two molecules (Fig 5A–5D). Similar interactions were not observed when sNPF was co-applied with other *Drosophila* neuropeptides, suggesting that the interaction of sNPF and PDF is specific. Nevertheless, the addition of TTX dampened the short-term response, suggesting that additional cells participate in the synergism between sNPF and PDF (Fig 5E–5H). Interestingly, *han* mutants lacking PDFR did not respond to PDF, sNPF or sNPF+PDF co-application (Fig 7A–7D). For sNPF, these results are puzzling, but since the rescue of PDFR in the IPCs only restored the response to PDF but not to sNPF, we conclude that sNPF does not act via PDFR. Still, we cannot completely exclude a cross-talk between PDFR and sNPFR1. For instance, there is evidence that GPCRs can engage in homo- or hetero-oligomeric complexes, resulting in cooperativity (reviewed in [90]). Alternatively, an interaction downstream of the receptors may occur, for example at the level of the signalosomes. PDFR and sNPFR associate with specific and different signalosomes that may have enhancing or opposing effects on cAMP levels [76–79,91]. However, further studies are required to investigate these possibilities using experimental settings that are closer to physiological conditions than bath applications of peptides. Interestingly, sNPF (produced in the s-LN$_v$s and in a subset of dorsal lateral neurons) and PDF interact on clock neurons and set the phase of their cytosolic Ca^{2+} rhythms according to neuron cluster [42]. PDF primarily regulates Ca^{2+} rhythms in the LN$_d$ and DN3 clusters, while sNPF orchestrates that of the DN1 [42]. Thus, the two signaling pathways act dynamically to facilitate the right timing of circadian neuronal activities. Similar complex regulation could also influence the seasonal clock system.

While the *Pdf* mRNA and protein do not cycle, it has been reported that PDF cycles at the nerve terminals with a circadian rhythm [39]. Thus, we presume that the daily rhythmic stimulation of the IPCs under normal summer conditions of warm days and long photoperiods maintains the expression of dILPs and suppresses dormancy. A simple model would have low temperatures and short photoperiods reducing the expression of PDF and sNPF from the sLNvs terminals, which might be expected to reduce IPC activation and enhance reproductive arrest levels. This could mean that the transcription/translation of these neuropeptides could be reduced under colder conditions, or alternatively, that their release was reduced from the sLNv terminal. This scenario might imply higher levels of PDF within the sLNv soma if it is sequestered there. Alternatively, the receptors for PDF and SNPF on the IPCs might be less sensitive to their ligands at lower temperatures, which would have the same effect on reproductive arrest. Future studies are required to examine the dynamic nature of PDF/SNPF and receptor expression under simulated winter conditions.

PDF and sNPF–most likely from the s-LN$_v$s can maintain *D. melanogaster*, originally a tropical species, in the reproductive state. However, it is intriguing that high-latitude *Drosophila* species such as *D. montana*, *D. littoralis*, *D. ezoana* and *D. virilis* lack PDF in the s-LN$_v$s [92–95]. These species have a high incidence of reproductive arrest even under long-day-lengths, an adaptation to the low temperatures even under summer photoperiods at these clines. For example, *D. ezoana* enters diapause when day-length falls below 16 hours [96]. Although we do not know whether the s-LN$_v$s of the high-latitude species still express sNPF, we speculate that the lack of PDF-signaling to the IPCs of these species might facilitate the

termination of the reproductive state under short-day condition, and induce ovarian arrest [97]. The role of the s-LN$_v$s as a source of PDF and sNPF may thus provide the entry point into the neuronal mechanism that allows *D. melanogaster* to detect the environmental conditions that predispose them to reproductive dormancy.

Materials and methods

Fly stock and Maintenance

Flies were reared at 23°C, 70% relative humidity, under 12-hour light/12-hour dark cycles (LD 12:12) on cornmeal standard food. The following, previously described fly strains were used: *Hu-S* Dutch natural population [37], *han^5304^* [59], UAS-*PDFR* [59], *gal1118 Gal4* enhancer trap [98], *R6*-Gal4 [70], UAS-*Epac1camps* [62], UAS-*hid* [99], UAS-*Pdf* [41], and *UAS-Den-Mark* [75]. *InsP3*-Gal4 was a gift from Michael J. Pankratz [73], *dilp2(p)*-Gal4 (*p, precocious*) was a gift from Eric J. Rulifson [21], UAS-*2xsNPF* [53] and UAS-*sNPFR1-DN* [54] were kindly provided Kweon Yu. Out of these lines, we newly combined *han^5304^*; *dilp2(p)*-Gal4, *han^5304^*;; UAS-*Epac1camps*, and *han^5304^*;UAS-*Epac1camps/CyO*;UAS-*PDFR*. The transgenic line *Pdf*-LexA,LexAop-*CD4::GFP_{11}/CyO*;UAS-*CD4::GFP_{1-10}/TM6b* for GRASP was a gift from François Rouyer. UAS-*OrkΔ-C* (designated as UAS-*Ork* [72]) and UAS-*Na^+ChBac* [69]) were gifts from Michael B. O'Connor. *Pdf^01^* mutants were backcrossed for 8 generations to a natural wild-type *ls-tim* line from The Netherlands [37]. The following lines were ordered from Bloomington Drosophila Stock Center: *Canton-S* wild-type strain (*#1*), *Crz_1*-Gal4 *(#51976)*, *Crz_2*-Gal4 *(#51977)*, *Elav^C155^*-Gal4 (designated as *elav*-Gal4, *#458*), *Pdf*-Gal4 (*#6900*), UAS-*CD8-GFP* (*BDSC #5137*), and *Oregon-R* (*#2376*; used as control for experiments with *han* mutant).

In order to use a control in which the specific transgene (Gal4 or UAS) was in the same condition of heterozygosis as in the experimental line, we have crossed all the parental lines to the *w^1118^* strain (generic genotype *w^1118^*;*P-element/+*). In *Drosophila*, two allelic variants of the *timeless* circadian clock gene (*s-tim/ls-tim*) were found to significantly influence reproductive arrest: *ls-tim* allele promotes reproductive quiescence at every photoperiod [37,38]. Considering this modulatory effect, controls were generated according to the *tim* allele of the UAS and Gal4 strains used in the experiments (see below for PCR *timeless* genotyping), with the help of *w^1118^; s-tim* (gift from Matthias Schlichting) and *w^1118^; ls-tim* (from our lab) lines that express either the *s-* or *ls-tim* isoform.

Dormancy assay

All fly stocks and crosses used for dormancy assays were maintained at 23°C in LD 12:12. Newly eclosed flies (within 5 h post-eclosion) were placed in plastic vials, and immediately subjected to 12°C in LD 8:16. After 11 days, flies were killed in abs EtOH, and ovaries of females were dissected in PBS. Dormancy levels were scored by considering the absence of yolk deposition in the ovarian follicles [7]. These data were presented as the proportion of females with ovarian arrest among all the dissected individuals. On average, 5 replicates of n>60 flies were dissected for each genotypes.

Immunocytochemistry

Flies were reared at 23°C in LD 12:12, and newly eclosed individuals were placed in short days (LD 8:16) at different temperatures (12, 18, 23°C) for 11 days. Females were collected at ZT1 (*Zeitgeber* Time 1, 1 h after light-on), and immediately fixed in 4% paraformaldehyde (PFA) in PBS for 100 min at room temperature (RT). After 3 washes in PBS, brains were dissected in ice-cold PBS, fixed in PFA 4% for 40 min at RT, and subsequently washed 6 times in PBS

containing 0.3% Triton X-100 (PBS-T). Next, samples were permeabilized in 1% PBS-T, followed by an overnight blocking step in 1% bovine serum albumin (BSA) in 0.3% PBS-T at 4°C. Afterwards, brains were incubated in primary antibody solution (diluted in 0.1% BSA, 0.3% PBS-T) for 3 days at 4°C. After 6 washes in 1% BSA in 0.3% PBS-T at RT, another blocking step was performed in 1% BSA in 0.3% PBS-T at 4°C, followed by hybridization with the secondary antibody (diluted in 0.1% BSA, 0.3% PBS-T) overnight at 4°C. The primary antibodies used in this study: mouse anti-GFP (1:500; Thermo Fisher Scientific), rabbit-anti-GFP (1:1000; A6455, Invitrogen) and anti-PDF (1:5000; mAb C7, Developmental Study Hybridoma Bank, donated by Justin Blau), rabbit anti-DILP2, anti-sNPF recognizing the sNPF propeptide (for both 1:2000; Jan A. Veenstra [100,101]). The secondary antibodies used: Alexa Fluor 488 (goat anti-mouse, 1:250) Cy3 (goat anti-rabbit, 1:500) (Thermo Fisher Scientific), DyLight488 (goat-anti-rabbit 1:250) and DyLight649 (goat anti-mouse, 1:250) (Jackson ImmunoResearch, Dianova). Staining was visualized adopting either a semi-confocal (Nikon Eclipse 80i equipped with a QiCAM Fast Camera using the Image ProPlus software) or confocal microscope (ZEISS LSM700 running ZEN Lite software or Leica SP8).

Live optical imaging in the insulin producing cells

To real-time monitor cAMP or Ca^{2+} concentration changes in the IPCs, live optical imaging was performed using the genetically encoded cAMP sensor, Epac1-camps [62] and the genetically encoded Ca^{2+} sensor GCaMP3.0 [82]. Relying on the UAS-GAL4 binary system [102], the sensors were expressed specifically in the IPCs (*dilp2(p)>Epac1-camps* or *dilp2(p)> GCaMP3.0*). Female flies, maintained at 25°C in LD 12:12, were anesthetized on ice before brain dissections in cold hemolymph-like saline (HL3 [103]) and mounted at the bottom of a cap of a plastic Petri dish (35x10 mm, Becton Dickenson Labware, New Jersey) in HL3 with the dorsal surface up. Brains were allowed to recover from dissection 15 min prior to imaging. Live imaging was conducted by using an epifluorescent imaging setup (VisiChrome High Speed Polychromator System, ZEISS Axioskop2 FS plus, Photometrics CoolSNAP HQ CCD camera, Visitron Systems GmbH) Visitron Systems GmbH) using a 40x dipping objective (ZEISS 40x/1.0 DIC VIS-IR). IPCs were brought into focus and regions of interest were defined on single cell bodies using the Visiview Software (version 2.1.1, Visitron Systems, Puchheim, Germany). Time-lapse frames were imaged with 0.2 Hz and 4x binning by exciting the CFP fluorophore of the cAMP sensor with 434/17 nm light or the GFP fluorescence of GCaMP3 with 488/10 nm light. For cAMP imaging, CFP and YFP emissions were separately detected using a Photometrics DualView2 beam splitter. After measuring baseline FRETs for ~100 s, substances were bath-applied drop-wise using a pipette, and imaging was performed for 1000 s. The neuropeptides used in this study were applied in a final concentration of 10 **μM** in 0.1% DMSO in HL3. The water-soluble forskolin derivate NKH477 (10 **μM**, Sigma Aldrich) or the cholinergic agonist carbamylcholine (1mM, Sigma Aldrich) served as positive controls in cAMP and Ca^{2+} imaging, respectively, while HL3 alone with 0.1% DMSO was used as negative control. In the case of tetrodotoxin (TTX) treatments, brains were incubated for 15 min in 2 **μM** TTX in HL3 prior to imaging and substances were co-applied together with 2 **μM** TTX. Inverse Fluorescence Resonance Energy Transfer (iFRET) was calculated over time according to the following equation: iFRET = CFP/(YFP-CFP*0.357) [62]. Thereby, raw CFP and YFP emission data were background corrected; in addition, YFP data were further corrected by subtracting the CFP spillover into the YFP signal, which was determined as 0.357 (35.7% of the CFP signal). Next, iFRET traces of individual neurons were normalized to baseline and were averaged for each treatment. Finally, maximum iFRET changes were calculated for individual neurons to quantify and contrast response amplitudes of the different treatments. The

following synthetic neuropeptides were used in this study: pigment dispersing factor (PDF: *NSELINSLLSLPKNMNDAa*; Iris Biotech GmbH), short neuropeptide F-1 (sNPF-1: *AQRSP SLRLRFa*; Iris Biotech GmbH), adipokinetic hormone (AKH: *pQLTFSPDWa*, NovoPro Bioscience), allatostatin-C (Ast-C: *pEVRYRQCYFNPISCF*, gift from Paul H. Taghert), Tachykinin 4 (DTK-4: *APVNSFVGMRa*, gift from Paul H. Taghert), dFMRFamide 4 (SDNFMRFa, gift from Paul H. Taghert).

Intracellular Ca^{2+} level

For Ca^{2+} imaging, brains expressed the GCamp3.0 sensor in the insulin producing cells (*dilp2 (p)>GCaMP3.0*) [104]. The preparation of the brain samples was the same as in the case of cAMP imaging, and the same microscope was used with a modified setup, measuring GFP fluorescence without a beam splitter. The cholinergic agonist carbamylcholine (1 mM CCh) was used to generate rapid Ca^{2+} increases (Nakai et al. 2001). After subtraction of background fluorescence, changes in fluorescence intensity were calculated for each ROI as $\Delta(F/F_0) = [(F_n—F_0)/F_0] \times 100$ with F_n as fluorescence intensity at time point *n* and F_0 as the baseline fluorescence calculated prior to the application of the different substances to the brain.

PCR for *timeless* genotyping

To ensure genetic homogeneity for the *tim* locus, between the experimental flies and their corresponding controls, all the strains used in this study were genotyped in order to identify the *tim* allele present in their genome (summarized in S1 Table). The genomic DNA was extracted from individual adult females (10 flies per genotype) by homogenizing them in 50 **μl** of extraction buffer (Tris HCl pH = 8.2 10 mM, EDTA 2 mM, NaCl 25 mM); after addition of 1 **μl** of Proteinase K (10 mg/ml) samples were incubated at 37˚C for 45 min, followed by 3 min at 100˚C. The *tim* region containing the polymorphic site was amplified using a reverse primer *(5'-AGATTCCACAAGATCGTGTT-3')* and two different forward primers (*ls-tim*: *5'-TGGAA TAATCAGAACTTTGA-3'*; *s-tim*: *5'-TGGAATAATCAGAACTTTAT-3')* that allow selective amplification of the different *tim* alleles [37].

qRT-PCR assays

Larvae of the following genotypes: *Act>sNPFR1-RNAi*, *Act>+* and *+>sNPFR1-RNAi*, were reared under standard conditions at 23˚C and LD12:12 until eclosion. Newly eclosed female flies were collected and subsequently exposed to low (12˚C) or high (23˚C) temperature and short photoperiod (8h:16hL:D) for 11 days. mRNA was isolated from whole bodies of 10 females. mRNA was reverse-transcribed with SuperScript II First-Strand Synthesis SuperMix (Invitrogen). PCRs were performed on a CFX96 Touch Real Time PCR Detector System (Bio Rad) with GoTaq qPCR Master Mix (Promega), using the following primers: *sNPFR- F*: 5'- *CGACCATCAGATGCACCA -3'*, *R*: 5'-*CGTCCGTCTCGTCTGTCC -3'*; *rp49 F*: 5'- *ATCGGT TACGGATCGAACAA-3'*, *R*: 5'- *GACAATCTCCTTGCGCTTCT-3'*. The results are shown as relative expression ratios obtained with the $2^{-\Delta\Delta Ct}$ method ± SEM. RP49 was used as reference. Results are shown in S2 Fig.

Statistics

Data were analysed with R statistical software (version 3.0.1, www.r-project.org) and plotted using GraphPad Prism 6 software. In the case of normally distributed data (Shapiro-Wilk normality test, p>0.05), statistical significance was tested by one- or two-way ANOVA with *post-hoc* Tukey's HSD tests, while data that were not normally distributed were analyzed by

Wilcoxon or Mann-Whitney test. In the case of multiple comparisons, raw p-values were further adjusted using Bonferroni correction, and these corrected p-values served as significance levels. When analyzing dormancy assays, all data were transformed to arcsine. For simplicity, figures in the *Results* section show untransformed data (dormancy, %).

Supporting information

S1 Table. The *timeless* background of the *Drosophila* strains used in this study, determined by genotyping PCR. *ls* = long and short allelic variant; s = short allelic variant.
(TIFF)

S2 Table. Numerical data on which each graph was based, and pertinent statistical significance values.
(XLSX)

S1 Fig. Genetic manipulation of the dorsal-lateral peptidergic neurons has no effect on dormancy. (A) Hypersensitization of DLPs through the expression of a bacterial sodium channel ($Crz_1 > Na^+ChBac$) does not alter quiescence levels (no difference from the Gal4 control). (B) Overexpression of sNPF in the DLPs does not influence the dormancy (no difference from the UAS control). Numbers within bars refer to the number of dissected females considered in the assays. Data are presented as mean ± SEM. ANOVA on arcsine transformations, followed by *post-hoc* Tukey HSD test. ***p<0.001, n.s. not significant.
(TIFF)

S2 Fig. qRT-PCR of dsRNAi knockdown of *sNPFR1* at 23˚C (A) and 12\C (B).
(TIFF)

Acknowledgments

Author Contributions

Conceptualization: Dóra Nagy, Christian Wegener, Ezio Rosato, Charalambos P. Kyriacou, Charlotte Helfrich-Förster, Rodolfo Costa.

Data curation: Dóra Nagy.

Formal analysis: Dóra Nagy, Gabriele Andreatta, Christiane Hermann-Luibl.

Funding acquisition: Charlotte Helfrich-Förster, Rodolfo Costa.

Investigation: Dóra Nagy, Paola Cusumano, Ane Martin Anduaga, Nils Reinhard, João Gesto, Christian Wegener.

Methodology: Gabriele Andreatta, Christiane Hermann-Luibl.

Supervision: Gabriella Mazzotta, Ezio Rosato, Charalambos P. Kyriacou, Charlotte Helfrich-Förster, Rodolfo Costa.

Writing – original draft: Dóra Nagy.

Writing – review & editing: Ezio Rosato, Charalambos P. Kyriacou, Charlotte Helfrich-Förster, Rodolfo Costa.

References

1. Tauber MJ, Tauber CA, Masaki S. Seasonal adaptations of insects. Oxford Univ Press USA. 1986; https://doi.org/10.1007/s11873-011-0171-2

2. Seasons of Life: The Biological Rhythms That Enable Living Things to Thrive and Survive: Russell G. Foster, Leon Kreitzman: 9780300167863: Amazon.com: Books [Internet].

3. Dunlap JC, Loros JJ. Making Time: Conservation of Biological Clocks from Fungi to Animals. Microbiol Spectr. 2017; https://doi.org/10.1128/microbiolspec FUNK-0039-2016

4. King AN, Sehgal A. Molecular and circuit mechanisms mediating circadian clock output in the Drosophila brain. European Journal of Neuroscience. 2018. https://doi.org/10.1111/ejn.14092 PMID: 30059181

5. Saunders DS, Lewis RD, Warman GR. Photoperiodic induction of diapause: Opening the black box. Physiological Entomology. 2004. https://doi.org/10.1111/j.1365-3032.2004.0369.x

6. Dolezel D. Photoperiodic time measurement in insects. Curr Opin Insect Sci. 2015; https://doi.org/10.1016/j.cois.2014.12.002

7. Saunders DS, Henrich VC, Gilbert LI. Induction of diapause in Drosophila melanogaster: photoperiodic regulation and the impact of arrhythmic clock mutations on time measurement. Proc Natl Acad Sci. 1989; https://doi.org/10.1073/pnas.86.10.3748 PMID: 2498875

8. Kenyon C, Chang J, Gensch E, Rudner A, Tabtiang R. A C. elegans mutant that lives twice as long as wild type. Nature. 1993; 366: 461–464. https://doi.org/10.1038/366461a0 PMID: 8247153

9. Tatar M, Chien S a, Priest NK. Negligible Senescence during Reproductive Dormancy in Drosophila melanogaster. Am Nat. 2001; https://doi.org/10.1086/321320 PMID: 18707322

10. Baumeister R, Schaffitzel E, Hertweck M. Endocrine signaling in Caenorhabditis elegans controls stress response and longevity. Journal of Endocrinology. 2006. https://doi.org/10.1677/joe.1.06856 PMID: 16899554

11. Hahn DA, Denlinger DL. Energetics of Insect Diapause. Annu Rev Entomol. 2011; https://doi.org/10.1146/annurev-ento-112408-085436 PMID: 20690828

12. Hahn DA, Denlinger DL. Meeting the energetic demands of insect diapause: Nutrient storage and utilization. Journal of Insect Physiology. 2007. https://doi.org/10.1016/j.jinsphys.2007.03.018 PMID: 17532002

13. Kubrak OI, Kučerová L, Theopold U, Nässel DR. The sleeping beauty: How reproductive diapause affects hormone signaling, metabolism, immune response and somatic maintenance in Drosophila melanogaster. PLoS One. 2014; https://doi.org/10.1371/journal.pone.0113051 PMID: 25393614

14. Kučerová L, Kubrak OI, Bengtsson JM, Strnad H, Nylin S, Theopold U, et al. Slowed aging during reproductive dormancy is reflected in genome-wide transcriptome changes in Drosophila melanogaster. BMC Genomics. 2016; 17: 50. https://doi.org/10.1186/s12864-016-2383-1 PMID: 26758761

15. Anduaga AM, Nagy D, Costa R, Kyriacou CP. Diapause in Drosophila melanogaster—Photoperiodicity, cold tolerance and metabolites. J Insect Physiol. 2018; 105: 46–53. https://doi.org/10.1016/j.jinsphys.2018.01.003 PMID: 29339232

16. Nagy D, Andreatta G, Bastianello S, Martín Anduaga A, Mazzotta G, Kyriacou CP, et al. A Semi-natural Approach for Studying Seasonal Diapause in Drosophila melanogaster Reveals Robust Photoperiodicity. J Biol Rhythms. 2018; https://doi.org/10.1177/0748730417754116 PMID: 29415605

17. Kimura KD, Tissenbaum HA, Liu Y, Ruvkun G. daf-2, an insulin receptor-like gene that regulates longevity and diapause in Caenorhabditis elegans. Science. 1997; 277: 942–946. PMID: 9252323

18. Sim C, Denlinger DL. Insulin signaling and the regulation of insect diapause. Front Physiol. 2013; 4: 189. https://doi.org/10.3389/fphys.2013.00189 PMID: 23885240

19. Sim C, Denlinger DL. Insulin signaling and FOXO regulate the overwintering diapause of the mosquito Culex pipiens. Proc Natl Acad Sci U S A. 2008; 105: 6777–6781. https://doi.org/10.1073/pnas.0802067105 PMID: 18448677

20. Schiesari L, Andreatta G, Kyriacou CP, O'Connor MB, Costa R. The insulin-like proteins dILPs-2/5 determine diapause inducibility in Drosophila. PLoS One. 2016; https://doi.org/10.1371/journal.pone.0163680 PMID: 27689881

21. Rulifson EJ, Kim SK, Nusse R. Ablation of insulin-producing neurons in flies: growth and diabetic phenotypes. Science. 2002; 296: 1118–1120. https://doi.org/10.1126/science.1070058 PMID: 12004130

22. Ikeya T, Galic M, Belawat P, Nairz K, Hafen E. Nutrient-dependent expression of insulin-like peptides from neuroendocrine cells in the CNS contributes to growth regulation in Drosophila. Curr Biol CB. 2002; 12: 1293–1300. PMID: 12176357

23. Slaidina M, Delanoue R, Gronke S, Partridge L, Léopold P. A Drosophila insulin-like peptide promotes growth during nonfeeding states. Dev Cell. 2009; 17: 874–884. https://doi.org/10.1016/j.devcel.2009.10.009 PMID: 20059956

24. Broughton S, Alic N, Slack C, Bass T, Ikeya T, Vinti G, et al. Reduction of DILP2 in Drosophila triages a metabolic phenotype from lifespan revealing redundancy and compensation among DILPs. PLoS One. 2008; 3: e3721. https://doi.org/10.1371/journal.pone.0003721 PMID: 19005568

25. Liu Y, Liao S, Veenstra JA, Nässel DR. Drosophila insulin-like peptide 1 (DILP1) is transiently expressed during non-feeding stages and reproductive dormancy. Sci Rep. 2016; 6: 26620. https://doi.org/10.1038/srep26620 PMID: 27197757

26. Shiga S, Numata H. The role of neurosecretory neurons in the pars intercerebralis and pars lateralis in reproductive diapause of the blowfly, Protophormia terraenovae. Naturwissenschaften. 2000; 87: 125–128. PMID: 10798197

27. Hamanaka Y, Yasuyama K, Numata H, Shiga S. Synaptic connections between pigment-dispersing factor-immunoreactive neurons and neurons in the pars lateralis of the blow fly Protophormia terraenovae. J Comp Neurol. 2005; 491: 390–399. https://doi.org/10.1002/cne.20712 PMID: 16175545

28. Shimokawa K, Numata H, Shiga S. Neurons important for the photoperiodic control of diapause in the bean bug, Riptortus pedestris. J Comp Physiol A Neuroethol Sens Neural Behav Physiol. 2008; 194: 751–762. https://doi.org/10.1007/s00359-008-0346-y PMID: 18546002

29. Jaramillo AM, Zheng X, Zhou Y, Amado DA, Sheldon A, Sehgal A, et al. Pattern of distribution and cycling of SLOB, Slowpoke channel binding protein, in Drosophila. BMC Neurosci. 2004; 5: 3. https://doi.org/10.1186/1471-2202-5-3 PMID: 15005796

30. Foltenyi K, Greenspan RJ, Newport JW. Activation of EGFR and ERK by rhomboid signaling regulates the consolidation and maintenance of sleep in Drosophila. Nat Neurosci. 2007; 10: 1160–7. https://doi.org/10.1038/nn1957 PMID: 17694052

31. Allada R, Chung BY. Circadian organization of behavior and physiology in Drosophila. Annu Rev Physiol. 2010; 72: 605–24. https://doi.org/10.1146/annurev-physiol-021909-135815 PMID: 20148690

32. Cavanaugh DJ, Geratowski JD, Wooltorton JRA, Spaethling JM, Hector CE, Zheng X, et al. Identification of a circadian output circuit for rest:activity rhythms in Drosophila. Cell. 2014; 157: 689–701. https://doi.org/10.1016/j.cell.2014.02.024 PMID: 24766812

33. Barber AF, Erion R, Holmes TC, Sehgal A. Circadian and feeding cues integrate to drive rhythms of physiology in Drosophila insulin-producing cells. Genes Dev. 2016; 30: 2596–2606. https://doi.org/10.1101/gad.288258.116 PMID: 27979876

34. Allen MJ. What makes a fly enter diapause? Fly (Austin). 2007; 1: 307–310.

35. Nässel DR, Kubrak OI, Liu Y, Luo J, Lushchak O V. Factors that regulate insulin producing cells and their output in Drosophila. Front Physiol. 2013; 4: 252. https://doi.org/10.3389/fphys.2013.00252 PMID: 24062693

36. Nässel DR, Vanden Broeck J. Insulin/IGF signaling in Drosophila and other insects: factors that regulate production, release and post-release action of the insulin-like peptides. Cell Mol life Sci C. 2016; 73: 271–290. https://doi.org/10.1007/s00018-015-2063-3 PMID: 26472340

37. Tauber E, Zordan M, Sandrelli F, Pegoraro M, Osterwalder N, Breda C, et al. Natural selection favors a newly derived timeless allele in Drosophila melanogaster. Science. 2007; 316: 1895–1898. https://doi.org/10.1126/science.1138412 PMID: 17600215

38. Sandrelli F, Tauber E, Pegoraro M, Mazzotta G, Cisotto P, Landskron J, et al. A molecular basis for natural selection at the timeless locus in Drosophila melanogaster. Science. 2007; 316: 1898–1900. https://doi.org/10.1126/science.1138426 PMID: 17600216

39. Park JH, Helfrich-Förster C, Lee G, Liu L, Rosbash M, Hall JC. Differential regulation of circadian pacemaker output by separate clock genes in *Drosophila*. Proc Natl Acad Sci U S A. 2000; 97: 3608–3613. https://doi.org/10.1073/pnas.070036197 PMID: 10725392

40. Helfrich-Förster C. Development of pigment-dispersing hormone-immunoreactive neurons in the nervous system of *Drosophila melanogaster*. J Comp Neurol. 1997; 380: 335–354. PMID: 9087517

41. Renn SC, Park JH, Rosbash M, Hall JC, Taghert PH. A pdf neuropeptide gene mutation and ablation of PDF neurons each cause severe abnormalities of behavioral circadian rhythms in Drosophila. Cell. 1999; 99: 791–802. https://doi.org/10.1016/S0092-8674(00)81676-1 PMID: 10619432

42. Liang X, Holy TE, Taghert PH. A series of suppressive signals within the *Drosophila* circadian neural circuit generates sequential daily outputs. Neuron. 2017; https://doi.org/10.1016/j.neuron.2017.05.007 PMID: 28552314

43. Yoshii T, Wülbeck C, Sehadova H, Veleri S, Bichler D, Stanewsky R, et al. The neuropeptide pigment-dispersing factor adjusts period and phase of *Drosophila*'s clock. J Neurosci Off J Soc Neurosci. 2009; 29: 2597–2610. https://doi.org/10.1523/JNEUROSCI.5439-08.2009 PMID: 19244536

44. Sheeba V, Fogle KJ, Kaneko M, Rashid S, Chou YT, Sharma VK, et al. Large Ventral Lateral Neurons Modulate Arousal and Sleep in Drosophila. Curr Biol. 2008; 18: 1537–1545. https://doi.org/10.1016/j.cub.2008.08.033 PMID: 18771923

45. Parisky KM, Agosto J, Pulver SR, Shang Y, Kuklin E, Hodge JJL, et al. PDF Cells Are a GABA-Responsive Wake-Promoting Component of the Drosophila Sleep Circuit. Neuron. 2008; 60: 672–682. https://doi.org/10.1016/j.neuron.2008.10.042 PMID: 19038223

46. Kim WJ, Jan LY, Jan YN. A PDF/NPF neuropeptide signaling circuitry of male Drosophila melanogaster controls rival-induced prolonged mating. Neuron. 2013; 80: 1190–1205. https://doi.org/10.1016/j.neuron.2013.09.034 PMID: 24314729

47. Shiga S, Numata H. Roles of PER immunoreactive neurons in circadian rhythms and photoperiodism in the blow fly, Protophormia terraenovae. J Exp Biol. 2009; 212: 867–877. https://doi.org/10.1242/jeb.027003 PMID: 19252004

48. Meuti ME, Stone M, Ikeno T, Denlinger DL. Functional circadian clock genes are essential for the over-wintering diapause of the Northern house mosquito, Culex pipiens. J Exp Biol. 2015; 218: 412–422. https://doi.org/10.1242/jeb.113233 PMID: 25653422

49. Ikeno T, Numata H, Goto SG, Shiga S. Involvement of the brain region containing pigment-dispersing factor-immunoreactive neurons in the photoperiodic response of the bean bug, Riptortus pedestris. J Exp Biol. 2014; 217: 453–462. https://doi.org/10.1242/jeb.091801 PMID: 24198258

50. Huybrechts J, De Loof A, Schoofs L. Diapausing Colorado potato beetles are devoid of short neuropeptide F I and II. Biochem Biophys Res Commun. 2004; 317: 909–916. https://doi.org/10.1016/j.bbrc.2004.03.136 PMID: 15081426

51. Cerstiaens A, Benfekih L, Zouiten H, Verhaert P, De AL, Schoofs L. Led-NPF-1 stimulates ovarian development in locusts. Peptides. 1999; 20: 39–44. https://doi.org/10.1016/S0196-9781(98)00152-1 PMID: 10098622

52. Schoofs L, Clynen E, Cerstiaens A, Baggerman G, Wei Z, Vercammen T, et al. Newly discovered functions for some myotropic neuropeptides in locusts. Peptides. 2001; 22: 219–227. PMID: 11179815

53. Lee K-S, You K-H, Choo J-K, Han Y-M, Yu K. Drosophila short neuropeptide F regulates food intake and body size. J Biol Chem. 2004; 279: 50781–50789. https://doi.org/10.1074/jbc.M407842200 PMID: 15385546

54. Lee K-S, Kwon O-Y, Lee JH, Kwon K, Min K-J, Jung S-A, et al. Drosophila short neuropeptide F signalling regulates growth by ERK-mediated insulin signalling. Nat Cell Biol. 2008; 10: 468–475. https://doi.org/10.1038/ncb1710 PMID: 18344986

55. Nässel DR, Enell LE, Santos JG, Wegener C, Johard HAD. A large population of diverse neurons in the Drosophila central nervous system expresses short neuropeptide F, suggesting multiple distributed peptide functions. BMC Neurosci. 2008; 9: 90. https://doi.org/10.1186/1471-2202-9-90 PMID: 18803813

56. Johard HAD, Yoishii T, Dircksen H, Cusumano P, Rouyer F, Helfrich-Förster C, et al. Peptidergic clock neurons in Drosophila: ion transport peptide and short neuropeptide F in subsets of dorsal and ventral lateral neurons. J Comp Neurol. 2009; 516: 59–73. https://doi.org/10.1002/cne.22099 PMID: 19565664

57. Kapan N, Lushchak O V., Luo J, Nässel DR. Identified peptidergic neurons in the Drosophila brain regulate insulin-producing cells, stress responses and metabolism by coexpressed short neuropeptide F and corazonin. Cell Mol life Sci C. 2012; 69: 4051–4066. https://doi.org/10.1007/s00018-012-1097-z PMID: 22828865

58. Shiga S, Davis NT, Hildebrand JG. Role of neurosecretory cells in the photoperiodic induction of pupal diapause of the tobacco hornworm Manduca sexta. J Comp Neurol. 2003; 462: 275–285. https://doi.org/10.1002/cne.10683 PMID: 12794732

59. Hyun S, Lee Y, Hong S-T, Bang S, Paik D, Kang J, et al. *Drosophila* GPCR Han is a receptor for the circadian clock neuropeptide PDF. Neuron. 2005; 48: 267–278. https://doi.org/10.1016/j.neuron.2005.08.025 PMID: 16242407

60. Lear BC, Merrill CE, Lin J-M, Schroeder A, Zhang L, Allada R. A G protein-coupled receptor, groom-of-PDF, is required for PDF neuron action in circadian behavior. Neuron. 2005; 48: 221–227. https://doi.org/10.1016/j.neuron.2005.09.008 PMID: 16242403

61. Mertens I, Vandingenen A, Johnson EC, Shafer OT, Li W, Trigg JS, et al. PDF receptor signaling in Drosophila contributes to both circadian and geotactic behaviors. Neuron. 2005; 48: 213–219. https://doi.org/10.1016/j.neuron.2005.09.009 PMID: 16242402

62. Shafer OT, Kim DJ, Dunbar-Yaffe R, Nikolaev VO, Lohse MJ, Taghert PH. Widespread receptivity to neuropeptide PDF throughout the neuronal circadian clock network of Drosophila revealed by real-time cyclic AMP imaging. Neuron. 2008; 58: 223–237. https://doi.org/10.1016/j.neuron.2008.02.018 PMID: 18439407

63. Im SH, Taghert PH. PDF receptor expression reveals direct interactions between circadian oscillators in *Drosophila*. J Comp Neurol. 2010; 518: 1925–1945. https://doi.org/10.1002/cne.22311 PMID: 20394051

64. Garczynski SF, Brown MR, Shen P, Murray TF, Crim JW. Characterization of a functional neuropeptide F receptor from Drosophila melanogaster. Peptides. 2002; 23: 773–780. PMID: 11897397

65. Mertens I, Meeusen T, Huybrechts R, De Loof A, Schoofs L. Characterization of the short neuropeptide F receptor from Drosophila melanogaster. Biochem Biophys Res Commun. 2002; 297: 1140–1148. PMID: 12372405

66. Cazzamali G, Saxild N, Grimmelikhuijzen C. Molecular cloning and functional expression of a Drosophila corazonin receptor. Biochem Biophys Res Commun. 2002; 298: 31–36. PMID: 12379215

67. Park Y, Kim Y-J, Adams ME. Identification of G protein-coupled receptors for Drosophila PRXamide peptides, CCAP, corazonin, and AKH supports a theory of ligand-receptor coevolution. Proc Natl Acad Sci U S A. 2002; 99: 11423–11428. https://doi.org/10.1073/pnas.162276199 PMID: 12177421

68. Carlsson MA, Enell LE, Nässel DR. Distribution of short neuropeptide F and its receptor in neuronal circuits related to feeding in larval Drosophila. Cell Tissue Res. 2013; 353: 511–523. https://doi.org/10.1007/s00441-013-1660-4 PMID: 23760890

69. Nitabach MN, Wu Y, Sheeba V, Lemon WC, Strumbos J, Zelensky PK, et al. Electrical hyperexcitation of lateral ventral pacemaker neurons desynchronizes downstream circadian oscillators in the fly circadian circuit and induces multiple behavioral periods. J Neurosci Off J Soc Neurosci. 2006; 26: 479–489. https://doi.org/10.1523/JNEUROSCI.3915-05.2006 PMID: 16407545

70. Hewes RS, Schaefer AM, Taghert PH. The cryptocephal gene (ATF4) encodes multiple basic-leucine zipper proteins controlling molting and metamorphosis in Drosophila. Genetics. 2000; 155: 1711–1723. PMID: 10924469

71. Gmeiner F, Kołodziejczyk A, Yoshii T, Rieger D, Nässel DR, Helfrich-Förster C. GABA(B) receptors play an essential role in maintaining sleep during the second half of the night in Drosophila melanogaster. J Exp Biol. 2013; 216: 3837–3843. https://doi.org/10.1242/jeb.085563 PMID: 24068350

72. Nitabach MN, Blau J, Holmes TC. Electrical silencing of Drosophila pacemaker neurons stops the free-running circadian clock. Cell. 2002; 109: 485–495. PMID: 12086605

73. Buch S, Melcher C, Bauer M, Katzenberger J, Pankratz MJ. Opposing effects of dietary protein and sugar regulate a transcriptional target of Drosophila insulin-like peptide signaling. Cell Metab. 2008; 7: 321–332. https://doi.org/10.1016/j.cmet.2008.02.012 PMID: 18396138

74. Kubrak OI, Lushchak O V., Zandawala M, Nässel DR. Systemic corazonin signalling modulates stress responses and metabolism in Drosophila. Open Biol. 2016; 6. https://doi.org/10.1098/rsob.160152 PMID: 27810969

75. Nicolai LJJ, Ramaekers A, Raemaekers T, Drozdzecki A, Mauss AS, Yan J, et al. Genetically encoded dendritic marker sheds light on neuronal connectivity in Drosophila. Proc Natl Acad Sci. 2010; https://doi.org/10.1073/pnas.1010198107 PMID: 21059961

76. Duvall LB, Taghert PH. The circadian neuropeptide PDF signals preferentially through a specific adenylate cyclase isoform AC3 in M pacemakers of Drosophila. PLoS Biol. 2012; 10: e1001337. https://doi.org/10.1371/journal.pbio.1001337 PMID: 22679392

77. Hong S-H, Lee K-S, Kwak S-J, Kim A-K, Bai H, Jung M-S, et al. Minibrain/Dyrk1a regulates food intake through the Sir2-FOXO-sNPF/NPY pathway in Drosophila and mammals. PLoS Genet. 2012; 8: e1002857. https://doi.org/10.1371/journal.pgen.1002857 PMID: 22876196

78. Chen W, Shi W, Li L, Zheng Z, Li T, Bai W, et al. Regulation of sleep by the short neuropeptide F (sNPF) in Drosophila melanogaster. Insect Biochem Mol Biol. 2013; 43: 809–819. https://doi.org/10.1016/j.ibmb.2013.06.003 PMID: 23796436

79. Vecsey CG, Pírez N, Griffith LC. The Drosophila neuropeptides PDF and sNPF have opposing electrophysiological and molecular effects on central neurons. J Neurophysiol. 2014; 111: 1033–1045. https://doi.org/10.1152/jn.00712.2013 PMID: 24353297

80. Kim J, Neufeld TP. Dietary sugar promotes systemic TOR activation in Drosophila through AKH-dependent selective secretion of Dilp3. Nat Commun. 2015; 6: 6846. https://doi.org/10.1038/ncomms7846 PMID: 25882208

81. Birse RT, Söderberg JAE, Luo J, Winther AME, Nässel DR. Regulation of insulin-producing cells in the adult Drosophila brain via the tachykinin peptide receptor DTKR. J Exp Biol. 2011; 214: 4201–4208. https://doi.org/10.1242/jeb.062091 PMID: 22116763

82. Tian L, Hires SA, Mao T, Huber D, Chiappe ME, Chalasani SH, et al. Imaging neural activity in worms, flies and mice with improved GCaMP calcium indicators. Nat Methods. 2009; 6: 875–881. https://doi.org/10.1038/nmeth.1398 PMID: 19898485

83. Ojima N, Hara Y, Ito H, Yamamoto D. Genetic dissection of stress-induced reproductive arrest in Drosophila melanogaster females. PLoS Genet. 2018; https://doi.org/10.1371/journal.pgen.1007434 PMID: 29889831

84. Selcho M, Millán C, Palacios-Muñoz A, Ruf F, Ubillo L, Chen J, et al. Central and peripheral clocks are coupled by a neuropeptide pathway in Drosophila. Nat Commun. 2017; 8: 15563. https://doi.org/10.1038/ncomms15563 PMID: 28555616

85. Holst B, Hastrup H, Raffetseder U, Martini L, Schwartz TW. Two active molecular phenotypes of the tachykinin NK1 receptor revealed by G-protein fusions and mutagenesis. J Biol Chem. 2001; 276: 19793–19799. https://doi.org/10.1074/jbc.M100621200 PMID: 11279104

86. Palanche T, Ilien B, Zoffmann S, Reck MP, Bucher B, Edelstein SJ, et al. The neurokinin A receptor activates calcium and cAMP responses through distinct conformational states. J Biol Chem. 2001; 276: 34853–34861. https://doi.org/10.1074/jbc.M104363200 PMID: 11459843

87. Kilts JD, Gerhardt MA, Richardson MD, Sreeram G, Mackensen GB, Grocott HP, et al. Beta(2)-adrenergic and several other G protein-coupled receptors in human atrial membranes activate both G(s) and G(i). Circ Res. 2000; 87: 705–709. PMID: 11029407

88. Söderberg JAE, Carlsson MA, Nässel DR. Insulin-Producing Cells in the Drosophila Brain also Express Satiety-Inducing Cholecystokinin-Like Peptide, Drosulfakinin. Front Endocrinol (Lausanne). 2012; 3: 109. https://doi.org/10.3389/fendo.2012.00109 PMID: 22969751

89. Klose M, Duvall LB, Li W, Liang X, Ren C, Steinbach JH, et al. Functional PDF Signaling in the Drosophila Circadian Neural Circuit Is Gated by Ral A-Dependent Modulation. Neuron. 2016; 90: 781–794. https://doi.org/10.1016/j.neuron.2016.04.002 PMID: 27161526

90. George SR, O'Dowd BF, Lee SP. G-protein-coupled receptor oligomerization and its potential for drug discovery. Nat Rev Drug Discov. 2002; 1: 808–820. https://doi.org/10.1038/nrd913 PMID: 12360258

91. Duvall LB, Taghert PH. E and M circadian pacemaker neurons use different PDF receptor signalosome components in Drosophila. J Biol. Rhythms 2013; 28 (4), 239–248. https://doi.org/10.1177/0748730413497179 PMID: 23929551

92. Bahn JH, Lee G, Park JH. Comparative analysis of Pdf-mediated circadian behaviors between Drosophila melanogaster and D. virilis. Genetics. 2009; 181: 965–975. https://doi.org/10.1534/genetics.108.099069 PMID: 19153257

93. Kauranen H, Menegazzi P, Costa R, Helfrich-Förster C, Kankainen A, Hoikkala A. Flies in the north: locomotor behavior and clock neuron organization of Drosophila montana. J Biol Rhythms. 2012; 27: 377–387. https://doi.org/10.1177/0748730412455916 PMID: 23010660

94. Hermann C, Saccon R, Senthilan PR, Domnik L, Dircksen H, Yoshii T, et al. The circadian clock network in the brain of different Drosophila species. J Comp Neurol. 2013; 521: 367–388. https://doi.org/10.1002/cne.23178 PMID: 22736465

95. Menegazzi P, Dalla Benetta E, Beauchamp M, Schlichting M, Steffan-Dewenter I, Helfrich-Förster C. Adaptation of Circadian Neuronal Network to Photoperiod in High-Latitude European Drosophilids. Curr Biol CB. 2017; 27: 833–839. https://doi.org/10.1016/j.cub.2017.01.036 PMID: 28262491

96. Vaze KM, Helfrich-Förster C. Drosophila ezoana uses an hour-glass or highly damped circadian clock for measuring night length and inducing diapause. Physiol Entomol. 2016; 41: 378–389. https://doi.org/10.1111/phen.12165 PMID: 27867253

97. Kyriacou CP. Evolution: Fruit Fly Clocks on the Edge. Curr Biol CB. 2017; 27: R227–R230. https://doi.org/10.1016/j.cub.2017.02.017 PMID: 28324740

98. Blanchardon E, Grima B, Klarsfeld A, Chélot E, Hardin PE, Préat T, et al. Defining the role of Drosophila lateral neurons in the control of circadian rhythms in motor activity and eclosion by targeted genetic ablation and PERIOD protein overexpression. Eur J Neurosci. 2001; 13: 871–888. PMID: 11264660

99. Zhou L, Schnitzler A, Agapite J, Schwartz LM, Steller H, Nambu JR. Cooperative functions of the reaper and head involution defective genes in the programmed cell death of Drosophila central nervous system midline cells. Proc Natl Acad Sci U S A. 1997; 94: 5131–5136. https://doi.org/10.1073/pnas.94.10.5131 PMID: 9144202

100. Veenstra JA, Agricola H-J, Sellami A. Regulatory peptides in fruit fly midgut. Cell Tissue Res. 2008; 334: 499–516. https://doi.org/10.1007/s00441-008-0708-3 PMID: 18972134

101. Johard HAD, Enell LE, Gustafsson E, Trifilieff P, Veenstra JA, Nässel DR. Intrinsic neurons of Drosophila mushroom bodies express short neuropeptide F: relations to extrinsic neurons expressing different neurotransmitters. J Comp Neurol. 2008; 507: 1479–1496. https://doi.org/10.1002/cne.21636 PMID: 18205208

102. Brand AH, Perrimon N. Targeted gene expression as a means of altering cell fates and generating dominant phenotypes. Development. 1993; 118: 401–15. https://doi.org/10.1101/lm.1331809 PMID: 8223268

103. Stewart BA, Atwood HL, Renger JJ, Wang J, Wu CF. Improved stability of Drosophila larval neuromuscular preparations in haemolymph-like physiological solutions. J Comp Physiol A. 1994; 175: 179–191. PMID: 8071894

104. Nakai J, Ohkura M, Imoto K. A high signal-to-noise Ca(2+) probe composed of a single green fluorescent protein. Nat. Biotechnol. 2001; 19(2): 137–41. https://doi.org/10.1038/84397 PMID: 11175727